SwN23

SWITCH DEVELOPMENT
PHASES I AND II

PROJECT 25-605
FINAL REPORT

S. Mercer

June 1974

Prepared for

Sandia Laboratories
Albuquerque, New Mexico

Prepared by

Physics International Company
2700 Merced Street
San Leandro, California 94577

CONTENTS

ILLUSTRATIONS

ILLUSTRATIONS (cont.)

ILLUSTRATIONS (cont.)

SECTION 1

INTRODUCTION

The switch development work reported here was supported by Sandia Laboratories, Albuquerque under Contract Number 14-1027. The work was performed using facilities at Physics International's San Leandro plant. Several important advances were made in the technology of multimegavolt gas switches. The chief accomplishments were:

1. Successful testing of a plastic switch envelope at a average field greater than 0.5 MV per inch on the plastic, about twice that in general use at present

2. Sub-nanosecond jitter in the breakdown of a 3 MV sulphur hexafluoride (SF_6) switch triggered by an external 250 kV pulse

3. Consistent production of multiple channels closely grouped within the switch

All of the above were demonstrated in a single pressurized SF_6 switch incorporating advanced and novel features. The switch is compact, of low inductance, simple to trigger, and can be economically produced in modest quantities. It should therefore be well suited to the new generation of fast risetime, very high current pulser systems being developed by Sandia, as part of a program to achieve fusion in the laboratory through the electron-beam-initiated heating of solid materials.

Work was also performed during this contract on multimegavolt triggered oil switches, again with encouraging results. The work on the gas switch is summarized in the following section. Full details of the experimental arrangements and procedures are given in Appendices 1 and 2 for both types of switches.

SECTION 2

GAS SWITCH DEVELOPMENT

2.1 TRIGGERED OPERATION--THEORY AND PRACTICE

The principle utilized is that of the field enhanced trigger electrode, Figure 1. The trigger electrode is of thin metal, with a sharp edge located in the region of high field between the main electrodes. During charging of the switch, the thin metal lies on the plane of a natural equipotential, Figure 1(a), from which the trigger pulse then rapidly displaces it, Figure 1(b). Triggering produces an increase of macroscopic electric field on one side of the electrode and, in addition, a large field enhancement at the sharp edge. Breakdown occurs as a streamer rapidly propagates from the edge.

Obtaining consistent low-jitter breakdown depends on making the total breakdown time small. The breakdown time in a gas switch of this type is largely associated with the early motion of the streamer while it is still close to the sharp edge and is in turn determined chiefly by the trigger pulse voltage and by the dimensions of the edge and of the critical streamer transit region. It follows, in particular, that as total switch voltages rise, the trigger voltage need not increase in proportion but instead can remain relatively fixed. At high voltages, this gives rise to the design known as the V/N switch, the name of which refers to the fact that the ratio of the total gap voltage to that between the trigger electrode and ground is a large number (N). The trigger electrode is physically and

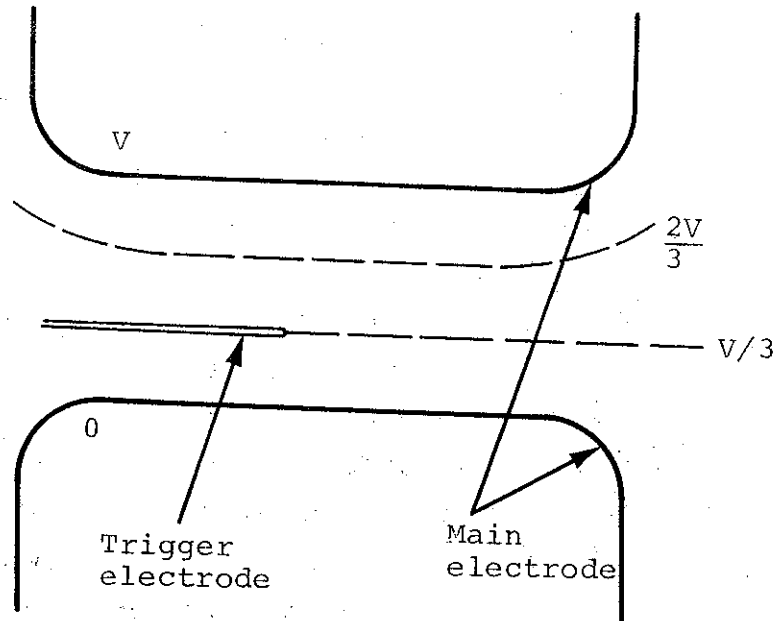

(a) No trigger pulse

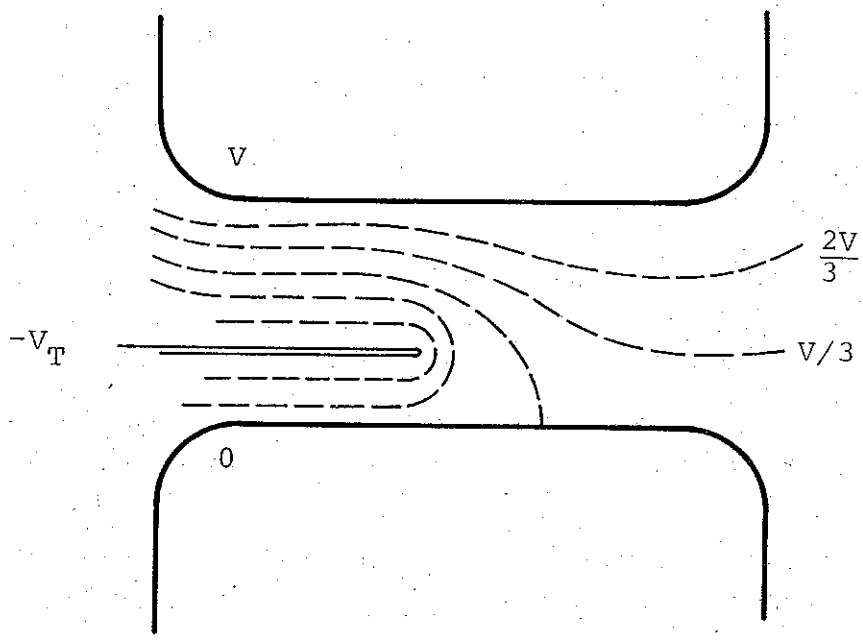

(b) With trigger pulse

Figure 1 Three electrode, field enhanced switch. For convenience of illustration, N = 3.

electrically close to ground, e.g., in a switch of several megavolts the trigger electrode is at a potential of only a few hundred kilovolts. The trigger pulse voltage has a comparable or somewhat greater magnitude, and inverts the trigger electrode potential with respect to ground.

As well as being appropriate in high voltage switches, the V/N approach works best with high field strengths in the gas, since a given field enhancement produces a greater degradation of breakdown voltage the higher the field. The use of SF_6 gas as the switch medium permits the field to be maximized conveniently, because the high molecular weight and low boiling point of SF_6 enable high densities to be obtained at modest pressures and at room temperature. The switch developed in the present work operates at 175 psig of SF_6.

The actual switch used is shown in Figure 2. The spacing between the main electrodes is 3 inches, to withstand about 3 MV at 175 psig SF_6. The trigger electrode is a 2.75-inch diameter disk, curved to follow the shape of an equipotential near the ground electrode. It is supported on a stem that passes through a hole cut in the ground electrode. The trigger electrode can be made to assume the desired potential by capacitive division, eliminating the need for balancing resistors. To achieve this, we use the fact that the trigger electrode potential will be that of the equipotential on which it lies. However this is only true if the trigger electrode capacitance, eliminated by cutting the hole in the ground electrode, is just made up by the capacitance of the stem to ground. The electrodes were designed to achieve such a balance with the trigger electrode about 0.2 inch from ground. The actual balance point was found by measuring the breakdown voltage of the switch with

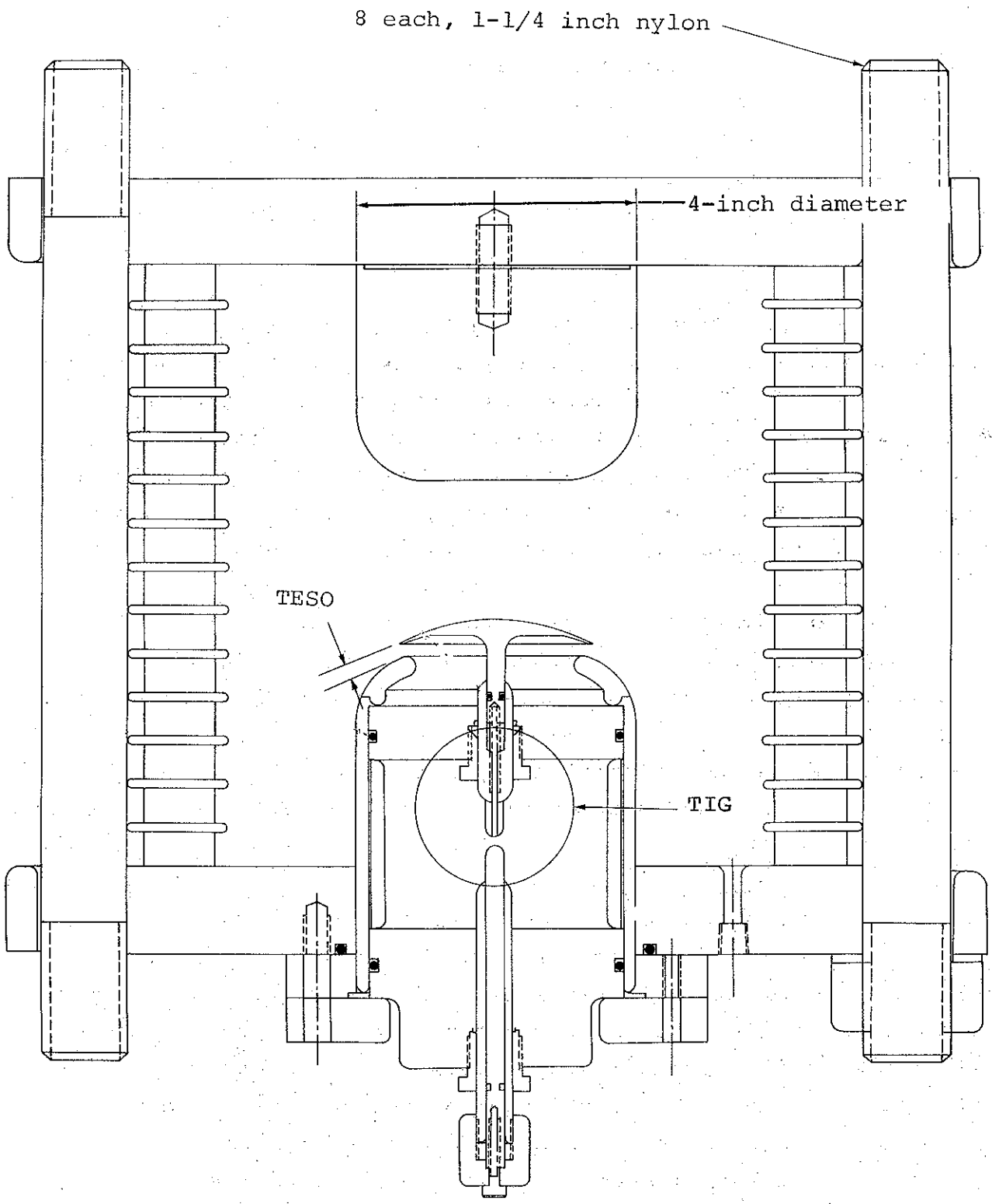

Figure 2 Partial assembly drawing of triggered gas switch.

different trigger spacings, Figure 3. Balance occurred at a spacing of about 0.25 inch when the breakdown voltage was a maximum and was equal to the previously determined value without the trigger electrode present. The trigger electrode potential at this distance is about 250 kV out of 3 MV, i.e., N ≈ 12 for this switch.

The circuit used to determine the switch jitter is shown in Figure 4. A Marx generator charges the switch to voltages up to and just over 3 MV. The Marx also charges the trigger line to about 250 kV. The trigger line is initially isolated from the trigger electrode by an isolation gap (built into the trigger electrode support) in order to avoid upsetting the capacitive balance of the switch. A self-closing gas switch inverts the voltage on the trigger line to produce the trigger pulse at the switch. This pulse must break down the isolation gap. If the charging waveform of the trigger line closely follows that of the trigger electrode, the isolation gap can be overvolted by a large ratio and will contribute little to the jitter. This was by no means the case in the present experiments, and the total jitter may have been partly or largely due to the isolation gap.

A typical set of data waveforms is shown in Figure 5. The times of closure of the trigger switch, the isolation switch, and the main gap are all clearly indicated on the same oscillogram. Typically, the isolation gap was found to breakdown in 10 nsec after the arrival of the trigger pulse, and the main switch after a further 12 nsec. The rms jitter of the main switch closure time was 0.9 nsec measured from breakdown of the isolation switch and 1.0 nsec measured from the arrival of the trigger pulse. This is consistent with most of the jitter being due to the isolation gap. The values include a contribution of 0.5 nsec probable maximum measurement error.

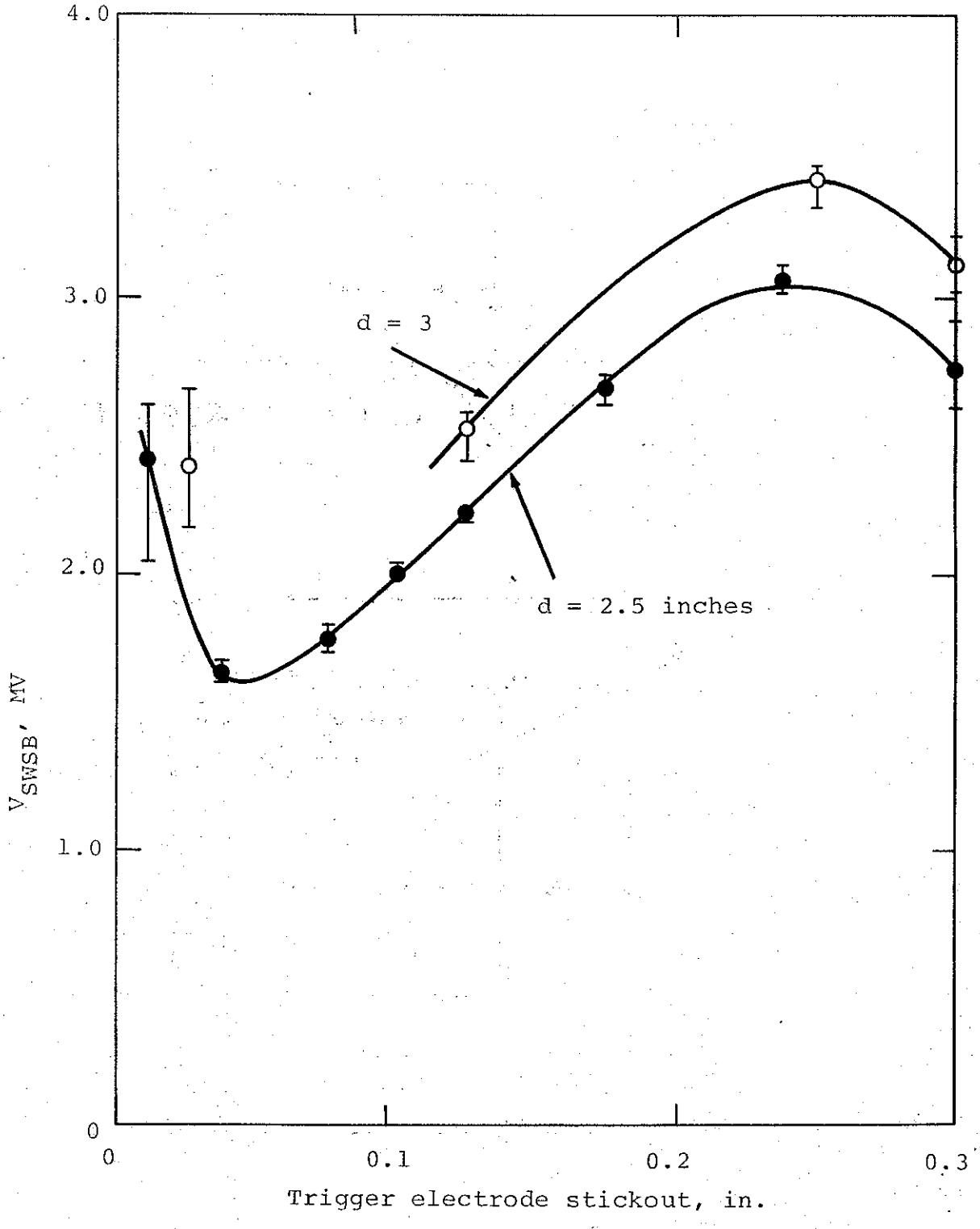

Figure 3 Switch breakdown voltage versus trigger electrode spacing for two values of main electrode spacing (d). Switch pressurized with 175 psig SF_6.

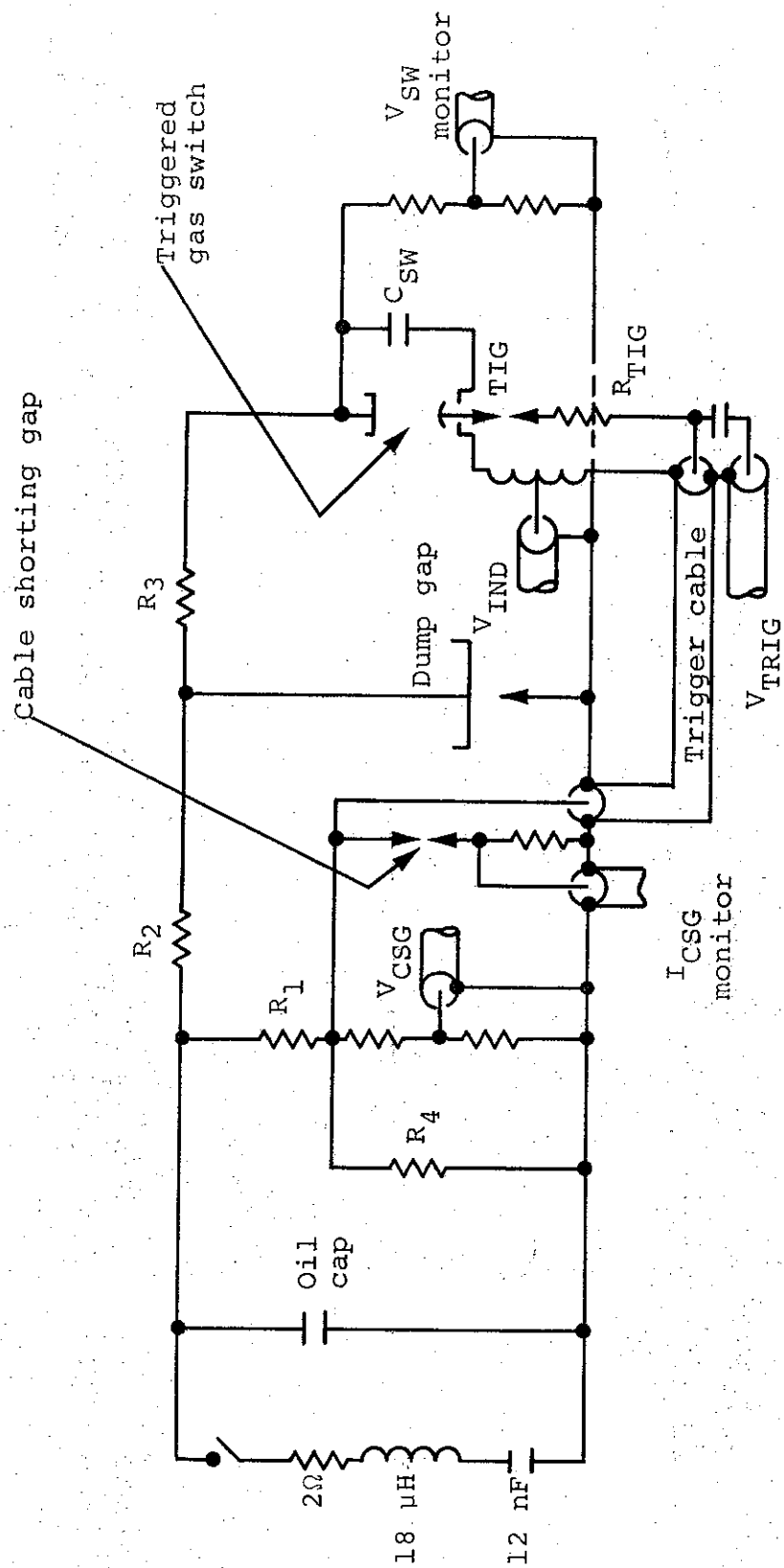

Figure 4 Basic schematic of oil tank layout for triggered gas switch tests.

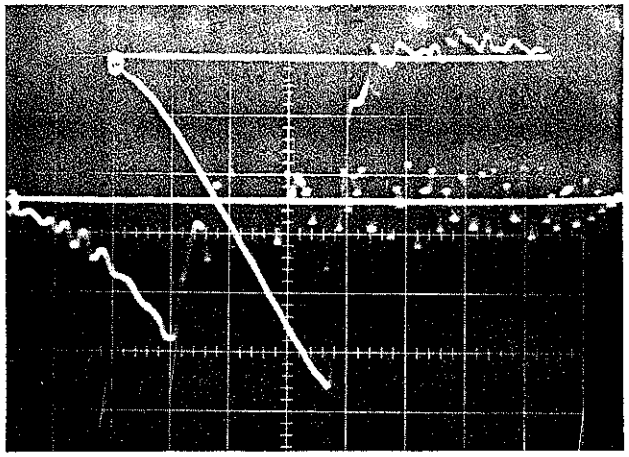

Top: V_{SW}

Vert. Sens: 0.5 MV/div

Horiz. Sens: 100 nsec/div

Bottom: V_{CSG}

Vert. Sens: 100 kV/div

Horiz. Sens: 100 nsec/div

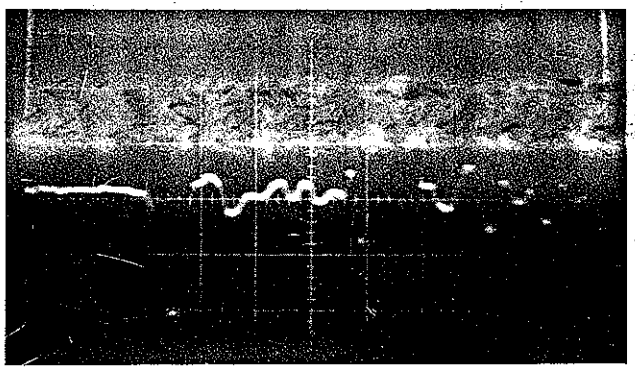

$I_{CSG} + V_{IND}$

Horiz. Sens: 10 nsec/div

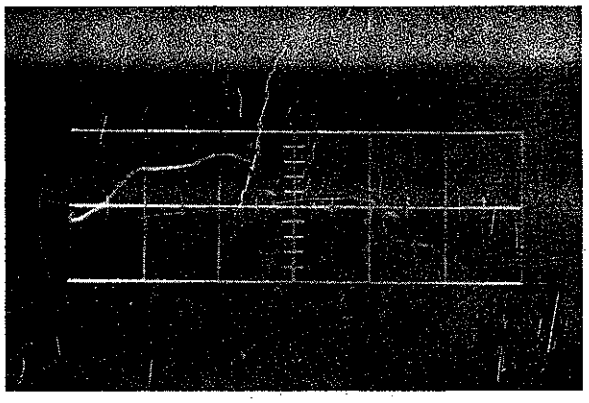

V_{TRIG}

Horiz. Sens: 5 nsec/div

Figure 5 Typical oscilloscope traces from which timing data are derived.

The calculated switch inductance with six channels is about 90 nH, which is in better agreement. In fact, because the monitor system risetime is about 2 to 5 nsec, the calculated inductance still appears high; however, this is probably due to the fact that the switch conductors to some extent form a part of the transmission line itself.

The existence of multiple channels having essentially zero transit time isolation from each other strongly indicates that the jitter of the main switch is of the order of a few tenths of a nanosecond at most, again suggesting that the isolation gap breakdown time may dominate the jitter. However, the isolation gap delay may possibly assist the multiple channel operation by sharpening the trigger pulse rise.

2.2 ENVELOPE DESIGN

Previous gas switches using a single continuous plastic wall to contain the gas have been subject to occasional tracking on the inside surface, necessitating refinishing or replacement of the plastic. This tracking is typically tolerated if it occurs only once in every few hundred pulses. In systems now contemplated by Sandia there may be one hundred switches, making such statistics unacceptable, and inductance and space considerations prohibit the relaxation of field levels to reduce the tracking probability by a large factor.

The switch, as shown in Figure 2, was designed with a pressure vessel composed of 14 Lucite rings, each 1/2 inch thick, separated by thin aluminum spacers. The use of a segmented envelope is based on the idea that when a track does initiate it shorts out only one segment, and if there are enough segments

the remainder will still withstand the voltage. Little energy is deposited in sparks that only short out one segment, and refinishing is unnecessary. A probability of 10^{-2} or higher can now be tolerated for a single segment track on a given shot, because total failure of the stack requires many segments to track simultaneously, and the probability of such essentially independent events coinciding now becomes many orders of magnitude lower. It was hoped that such a design might operate safely at fields higher than those commonly used, which are of the order of 250 kV/inch.

Tests were first conducted on individual insulator segments of various designs. The chief conclusions from these tests were that fields of 600 to 900 kV per inch are required to produce tracking on the inside (gas) interface; that a straight gas interface normal to the metal spacers gave a result at least as good as any other shape tried; that careful design of the outside (oil) interface is required to reach these fields; that even given good design, the limiting failures may still occur at the oil interface or at O-ring seals in the plastic rather than the gas interface; that Lexan degrades with even low energy tracks on the gas interface, while Lucite actually becomes better.

Based on these results, the design shown in Figure 2 was successfully adopted. It withstood 3.75 MV, without failure corresponding to a maximum field of about 600 kV per inch including 10 to 12 percent field enhancement. The average field is more than twice that quoted earlier as typical of single insulator switches. Occasional tracking of individual segments was observed to occur, showing that operation was in accordance with the design principles. The results obtained with single insulators show that still higher fields might be safely achieved; though observation of complete flashover in a 12-segment poorly graded switch at 3 MV indicates that further work is necessary to put these into useful practice.

Following the jitter test, the switch was installed at one end of a 20 nsec, 60 ohm pulse line. One objective of this test was to subject the switch to the current and charge appropriate to its use in a real application of interest. This objective was more than fulfilled, since in this test the line was allowed to ring through the switch.

A more important objective was to measure the switch risetime. The waveform in Figure 6 was obtained from a capacitive divider in the pulse line and shows a 10 to 90 percent risetime of just over 3 nsec. This corresponds to a switch inductance of approximately 85 nH, compared to about 150 nH calculated and assuming a single arc channel. This discrepancy is explained by Figure 7, which shows that from four to eight channels were regularly obtained.

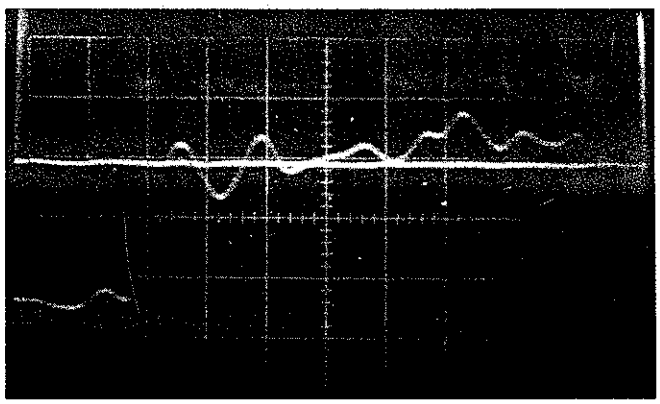

5 nsec/div

Figure 6 Trace from a capacitive divider pulse line voltage when switching a 60-ohm line.

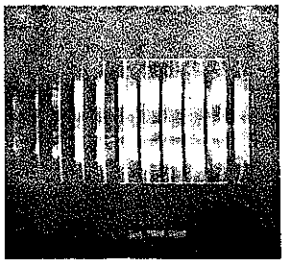

2.79 MV

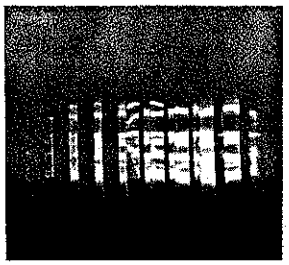

2.60 MV

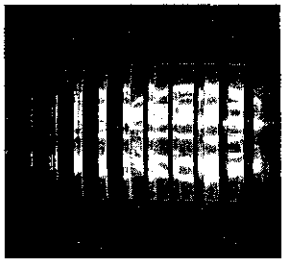

2.81 MV

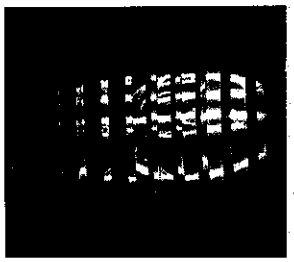

2.34 MV

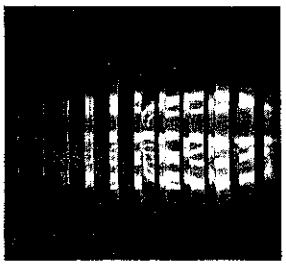

2.65 MV

2.0 MV

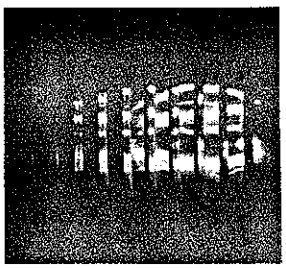

1.92 MV
(self-fire)

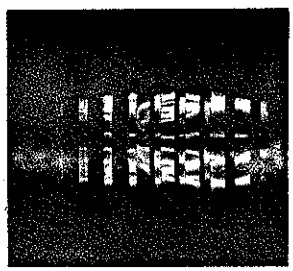

2.32 MV

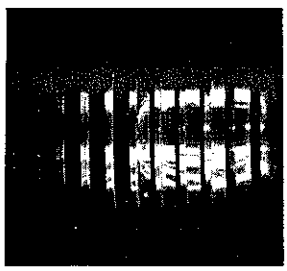

2.67 MV

Figure 7 A sequence of openshutter photographs of the gas switch showing multichannel switching. The peak switch voltage is listed.

APPENDIX A

GAS SWITCH TESTING

SECTION A-1

INTRODUCTION

This report presents the results of the experimental efforts by Physics International Company under contract to Sandia Laboratories for development of a gaseous dielectric switch to operate in an external oil environment.

Gaseous dielectric switch testing began with determination of the voltage flashover values of a single segment insulator of a proposed segmented (multistage) envelope. The pulse charge voltage was derived from a 29-stage air Marx. Conditioned holdoff values of 440 kV for the 1/2-inch-thick insulator (~ 350 kV/cm) for a gas pressure of 120 psig SF_6 were demonstrated for an equivalent 1-cos ωt waveform rising to peak in 400 nsec. The upper limits were generally set by breakdown through the body from an O-ring groove edge.

A multistage segmented envelope was tested for voltage holdoff in the oil tank using the 39-stage Marx. A stack of 12 segments without internal electrodes flashed at average envelope fields of 160 kV/cm to 190 kV/cm at 120 psig SF_6. This is about one-half the value for a single segment. Total holdoff voltage was increased by adding two stages, increasing the pressure and adding field shaping electrodes to the end plates. Fields of 220 kV/cm at 175 psig SF_6 were sustained without flashover.

In Phase II, the multistage segmented envelope gas switch structure was modified to become a triggered switch through the addition of V/n trigger electrode assembly which included a built-in trigger isolation gap (TIG). The self-break of the switch was measured as a function of trigger electrode stickout (TESO) for electrode spacings of 2.5 and 3.0 inches and found to be near 3.4 MV for the 3-inch spacing and a TESO value of 0.25 inches.

Jitter measurements of the triggered switch with 300-ohms isolation from the Marx system, but with substantial self-capacitance due to the field shaping electrodes, gave a value of $\sigma \leqslant 0.9$ nsec.

A capacitive monitor indicated a falltime of less than 3 nsec (10 to 90 percent) for the switch dumping a $\sim$ 60 ohm oil line. Multiple channel switching was observed by open-shutter photography.

SECTION A-2

GAS SWITCH TESTING--PHASE I

Gas switch testing in Phase I was conducted in two parts. First a single section of a proposed segmented (multistage) envelope of a gas switch was tested to determine the limits of voltage holdoff for Lucite and Lexan. These materials were chosen for their transparency and their reasonable mechanical properties. Based on the results, a segmented envelope of Lucite was assembled and tested for voltage holdoff capability.

A.2.1 SINGLE SEGMENT INSULATOR TESTS

Testing of single segment insulators began with the test fixture shown in Figure A-1. A scale section of the envelope and grading rings is given in Figure A-2. A basic schematic of the test setup is given in Figure A-3.

The test fixture was placed in a steel tank approximately 4 feet wide by 8 feet long with the axis of the envelope parallel to the tank axis and the nearest Lucite plate (ground side) approximately 6 inches from the tank end. The fixture was set on a 4-inch-thick Lucite sheet. The fixture, monitor, and a portion of the series resistor were covered with insulating oil. After each assembly, the gas enclosure was evacuated and backfilled with SF_6 supplied directly from a gas bottle.

d.

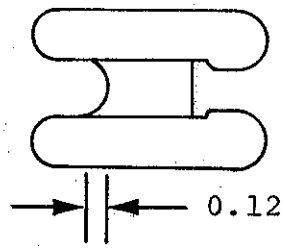

e.

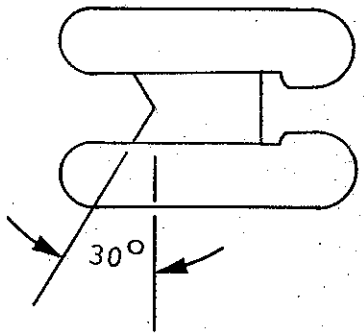

f.

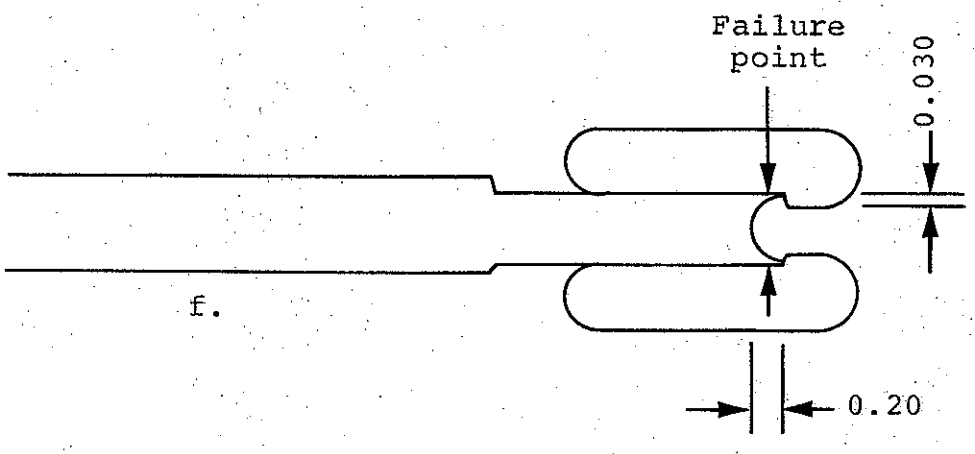

Figure A-2 (Continued).

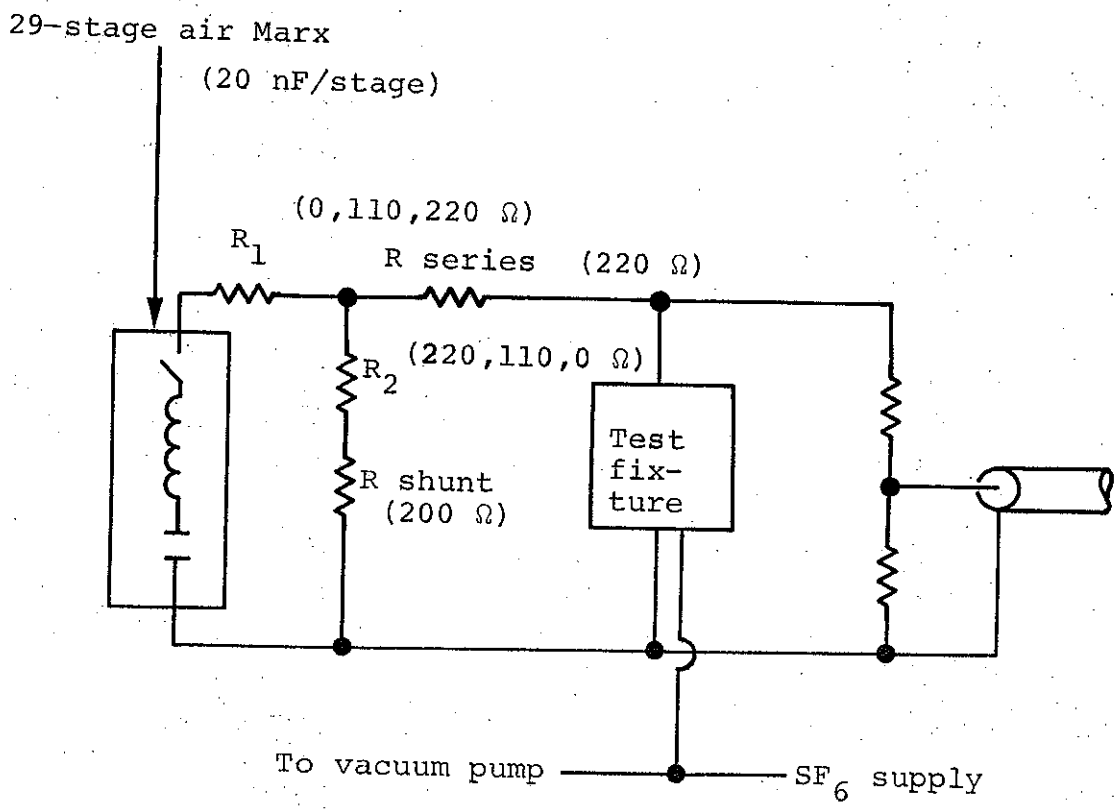

Figure A-3 Basic schematic diagram of single insulator gas envelope tests.

The waveform of Figure A-4 was obtained after a series inductance was added to the Marx generator to slow the risetime and smooth the pulse shape. The amount of voltage applied to the test insulator was determined by the Marx charge voltage and the voltage division ratio set by the resistor network. Approximately 80 percent of the voltage at the output of R_1 appeared on the insulator as a result of (1) the resistive division of the series resistor and the monitor and (2) the capacitive loading of the test fixture. R_1 and R_2 together consisted of two 110-ohm resistors so that the resistance values shown were available with the exception that one must be zero if the other was 220 ohms. The Marx charge voltage and the values of R_1 and R_2 were varied in order to cover the entire voltage range of the tests.

The effect on the output waveform of varying the resistance values was noticeable but was not considered a significant change. In general the series resistance was maintained as large as practical in order to limit the current in the event the insulator should flash over.

Early in testing, relatively few oscilloscope traces were overlaid, but as familiarity with the system increased, it became possible to superimpose as many as 95 traces on a picture. In addition to recording monitor traces in order to measure the voltage and look for flashover, the operators visually observed the test of each shot.

The test waveform was estimated to be roughly equivalent to a 1 minus cos ωt waveform rising in 400 nsec to peak. Any breakdown at any point on the trace or as visually observed was considered a failure for that shot regardless of location in time, even though as shown by oscilloscope traces, some occurred so late in the waveform that the insulator would have held for a fast pulse charge.

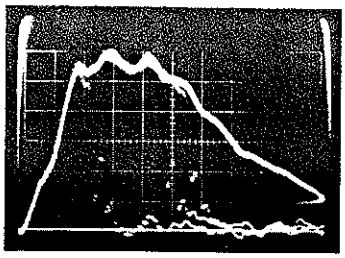

Vertical: 46 kV/div
Horizontal: 50 nsec/div

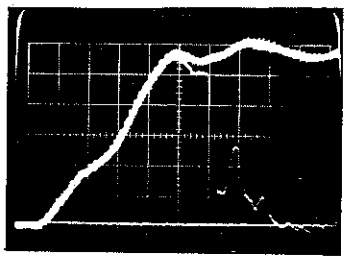

Horizontal: 20 nsec/div

Figure A-4 Shots 47 to 56 of Insulator 1 test. Three visual breaks were observed.

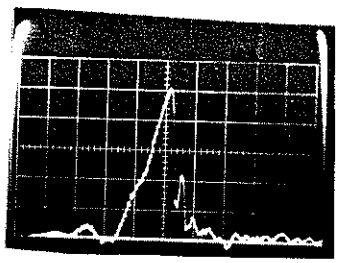

Vertical: 46 kV/div
Horizontal: 50 nsec/div
p = 120 psig SF_6

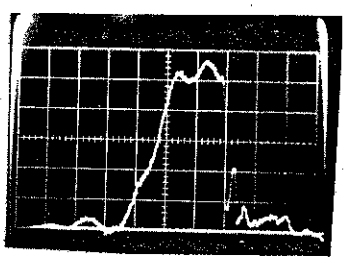

Figure A-5 Initial shots on Insulator No. 1.

The first test insulator (Figure A-22) was a circular Lucite ring 0.500 inch thick with inner and outer diameters of 10 and 12 inches, respectively. An uncounted number of shots was made in setting up the system. The pressure of the SF_6 gas was lowered to 30 psig and flashover occurred at 230 kV where the waveform was a nearly linear ramp of 80 nsec duration to break. Similar results occurred at 60 and 90 psig. At 120 psig, flashover occurred 80 nsec later (see Figure A-5) on the first shot, but did not occur on the succeeding two shots. The following shot was arbitrarily chosen as the first shot and the data for the remaining tests is tabulated in Table A-1. For all remaining tests the pressure was maintained constant at 120 psig except in the testing of insulator No. 9, a solid disk.

The tabulated data gives the envelope (test) number, the dc charge voltage of the Marx, the maximum measured envelope voltage, the calculated field at the gas-envelope interface, the field in the oil between the aluminum rings, the number of shots and breakdowns, and in some cases, the running total of shots and breakdowns. The field calculations neglect entirely any field enhancement, and particularly on the oil side the listed value is the lowest possible.

Test No. 1 was characterized by the apparent ability of the envelope to condition following flashover. A large step in voltage from 262 kV to 348 kV resulted in flashover on 20 consecutive shots. The voltage was lowered to 320 kV to look for conditioning and recovery, with positive results. With the voltage raised again to 342 kV, breakdown occurred on 50 out of 52 shots, i.e., there was no conditioning. Pulsing was stopped due to a gas leak and an observation was made that the envelope had tracked at the oil interface as well as on the gas interface. Dismantling for closer inspection disclosed a minimum of 40 tracks

TABLE A-1 Single insulator flashover test data. (All pressures are 120 psig SF_6 except for No. 9, atmospheric air on two sides of a solid disk.)

Insulator No.	V_{DC} (kV)	V_{SW} (kV)	V_{GAS} (kV/cm)	V_{OIL} (kV/cm)	Number of Tests	Breaks	Running Totals Number of Tests	Running Totals Breaks	Failure Mode
1	30	262	206	275	3	3	3	3	
					1	0	4	3	
					6	3	10	6	
					5	0	15	6	
					10	1	25	7	
					1	1	26	8	
					10	3	36	11	
					10	1	46	12	
					10	3	56	15	
					10	3	66	18	
					10	5	76	23	
					10	1	86	24	
					40	0	126	24	
	40	348	274	365	20	20			
	35	320	251	336	10	5	10	5	
					10	4	20	9	
					10	2	30	11	
					10	1	40	12	
					10	1	50	13	
					10	0	60	13	
					2	1	62	14	
	38	342	270	359	10	8	10	8	
					42	42	52	50	a, b
2	30	237	187	249	1	1	1	1	
		247	194	259	2	2	3	3	b
3	25	232	183	244	7	0	7	0	
					6	6	13	6	c
4	25	245	193	257	950	0	950	0	
		241	190	252	50	0	1000		
	30	273	215	287	225	0	1225		
	32	290	228	304	240	0	1465		
	33				335	0	1800		
	33	386	225	300	65		1865		
	37	312	246	328	10	0	1875		
	37	345	272	362	578	0	2453		

TABLE A-1 (cont.)

Insulator No.	V_{DC} (kV)	V_{SW} (kV)	V_{GAS} (kV/cm)	V_{OIL} (kV/cm)	Number of Tests	Breaks	Running Totals Number of Tests	Running Totals Breaks	Failure Mode
	30	330	260	346	5	0	2458	0	
	32	341	269	358	20	0	2478		
	35	374	294	393	29	0	2507		
						0			
	32	360	284	378	20	0	2527		
	35	400	318	422	25	0	2552		
	37	425	335	446	20	0	2572		
	30	403	317	423	1	0	2573		
	32	435	343	457	1	0	2574		
	34	464	365	487	1	0	2575		
	36	483	380	507	1	1	2576	1	
	26	393	309	413	2	0	2578		
	28	420	331	441	5	1	2583	2	
					7	5	2590	7	
					93	0	2683	7	
	30	440	346	462	4	2	2687	9	
					96	0	2787	9	
	32	468	369	491	2	1	2788	10	a
5	28	304	239	319	15	14			d
5a	24	198	156	208	6	0	6	0	
					94	1	100	1	
	26	212	167	226	100	0	200	1	
	28	217	171	228	100	0	300	1	
	30	223	176	234	100	0	400	1	
	32	231	182	243	5	0	405	1	
	34	242	191	254	10	0	415	1	
	34	267	210	280	29	3	444	4	
	30	198	156	208	1	1	445	5	
	26	181	143	190	1	1	446	6	d

TABLE A-1 (cont.)

Insulator No.	V_{DC} (kV)	V_{SW} (kV)	V_{GAS} (kV/cm)	V_{OIL} (kV/cm)	Number of Tests	Breaks	Running Totals Number of Tests	Running Totals Breaks	Failure Mode
6	24	220	173	231	5	1	5	1	
					21	0	26	1	
	24	220	173	231	100	1	126	1	
	26	242	190	254	100	0	226	1	
	28	245	193	257	100	0	326	1	
	30	253	199	266	100	0	426	1	
	32	270	213	283	11	1	437	2	
					89	0	526	2	
	34	280	220	294	100	0	626	2	
	26	312	248	328	100	0	726	2	
	28	330	260	346	100	0	826	2	
	30	343	270	360	100	0	926	2	
	32	359	282	377	5	1	5	1	
					8	2	13	3	
					5	1	18	4	
					10	4	28	8	
					25	0	53	8	
					3	3	56	11	
					102	0	158	11	
	34	373	294	392	5	5			
					10	0			
	34	380	300	399	2	2			
					2	0	4	2	
					3	3	7	5	
					22	0	29	5	
					1	1	30	6	a
7	24	225	177	236	100	0	100	0	
	28	253	199	266	100	0	200		
	32	272	214	286	100	0	300		
	34	286	225	300	100	0	400		
	26	308	243	323	100	0	500		
	30	330	260	346	100	0	600		
	32	354	279	372	100	0	700		
	34	390	307	409	16	1	716	1	a

TABLE A-1 (cont.)

Insulator No.	V_{DC} (kV)	V_{SW} (kV)	V_{GAS} (kV/cm)	V_{OIL} (kV/cm)	Number of Tests	Breaks	Running Totals Number of Tests	Running Totals Breaks	Failure Mode
8	24	247	194	259	100	0	100	0	
	28	272	214	286	100	0	200		
	32	294	231	309	25	0			
					1	1	226	1	
					1	0	227		
					1	1	228	2	
					72	0	300		
	34	300	236	315	100	0	400		
	26	330	260	246	100	0	500		
		321	253	337	20	0	520		
	30	364	287	382	5	5	525	7	
	26	332	261	349	20	0	545		
	28	342	270	359	86	0	631		
					1	1	632	8	b, a
					3	0	635		
					1	1	636	9	
					9	0	645		
	28	359	283	377	21	0	666		
	30	378	298	397	44	0	710	10	
9	24	215	169	226	100	0	100	0	
	28	250	197	262	100	0	200		
	30	260	205	273	100	0	300		
	32	267	210	280	100		400		
	26	320	252	336	100		500		
	30	355	280	373	50		550		
	32	360	283	378	30		580		
	26	290	228	304	5		585		
	30	344	271	361	110		695		
	32	362	285	380	100		975		
	34	385	303	404	50		845		

TABLE A-1 (cont.)

Insulator No.	V_{DC} (kV)	V_{SW} (kV)	V_{GAS} (kV/cm)	V_{OIL} (kV/cm)	Number of Tests	Breaks	Running Totals Number of Tests	Running Totals Breaks	Failure Mode
	36	417	328	438	100	0	945		
	38	171	135	180	1	1	946	1	c
10	24	170	133	178	100	0	100		
	28	197	155	207	100	0	200		
	30	210	166	220	100	0	300		
	32	221	174	232	50	0	350		
	34	234	185	246	100	1	450	1	
	26	240	189	252	100	4	550	5	
	30	267	210	280	10	10	560	15	d

Note:
- a - failure at "O"-ring groove
- b - oil surface tracking
- c - oil and body breakthrough
- d - gas surface tracking

on the oil interface. The gas leak was caused by fracture of the envelope past the O-ring groove. All of the gas-side tracks were in the lower half of the insulator and appeared to preferentially start from the positive ring. A few bits of Teflon tape used to make a pipe thread seal were found in the ring but could not be directly associated with the tracks. Hindsight showed that the difference in oil and gas-side tracking could be distinguished visually in most cases.

Envelope No. 2 was identical to No. 1. It held at 190 kV but failed 3 successive shots, one at 237 kV and two at 247 kV. On the third shot the envelope tracked on the exterior oil surface near the top.

Envelope No. 3 (Figure A-2b) was an attempt to bring the oil-envelope interface into a region of weaker fields. After holding at 232 kV for 6 shots, the insulator failed by tracking through at the insulator step.

A decision was made to abandon the step in the aluminum rings as a mechanical stop and the No. 2 insulator was machined to remove 0.25 inch from the outer diameter as shown in Figure A-2c. One internal track was found and polished out before assembly as insulator No. 4. After 1000 shots near 245 kV, the voltage was raised in steps until 20 shots at 425 kV gave a total of 2572 shots without breakdown. The voltage on the following 4 shots were respectively 403, 435, 464,and 483 kV with flashover occurring at peak on the last shot. (See Figure A-6.) Starting the next day, the voltage was lowered to 393 kV for 2 shots, then raised to 420 kV where flashover occurred on 6 of 12 shots, but then the envelope held for 93 successive shots. At 440 kV, it flashed 2 of the first 4 shots and held for 96 more.

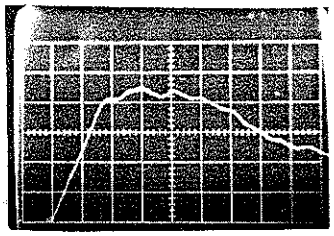

Vertical: 110 kV/div
Horizontal: 50 nsec/div

Figure A-6 Successive shots on Insulator No. 4 (straight sided Lucite) at 30, 32, 34 and 36 kV/div.

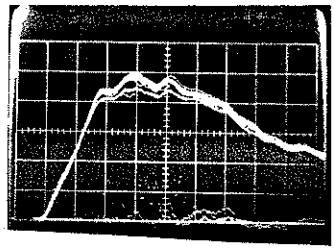

Shots 1 to 5 at 34 kV dc

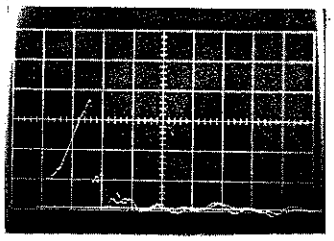

Shots 6 to 39 at 34 kV dc
flashed on last 3 shots

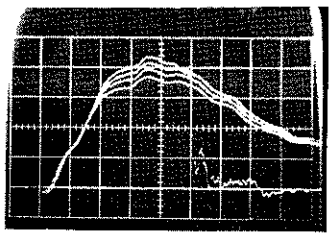

Flashed at 30 kV dc
Flashed at 26 kv dc

Figure A-7 Lexan ring showing degradation following initial flashover. All vertical deflections are 55 kV/div; all horizontal deflections are 50 nsec/div.

At 464 kV, the envelope held for 1 shot and failed on the second by sustaining an arc through the body from the inner edges of the O-ring groove.

Insulator No. 5 was made from Lexan to be similar in dimension to No. 4. The first shot was at 304 kV and held, but flashed on the next shot. Breakdown occurred at successively lower voltages as more attempts were made. Examination of the ring disclosed a single track mark of much greater damage than shown by the Lucite.

The envelope was remachined on the inner surface to remove all trace of tracking and retested as insulator No. 5a to a maximum of 267 kV where after initial flash, the same decreasing hold-off ability and tracking damage was found. The trace records for the higher voltage shots are shown in Figure A-7.

Lexan was abandoned in order to investigate the effect of shaping the inner envelope surface. Insulator No. 6 was machined from Lucite to have a concave surface on the gas side as shown in Figure A-2d. The gas surface was more prone to tracking than the straight surface of No. 4, but failure was by volume breakdown from the inner edge of the O-ring groove at 380 kV.

Insulator No. 7 was also of Lucite with a concave chevron bevel as shown in Figure A-2e. No flashing was observed prior to failure by volume breakdown from the O-ring groove edge on the sixteenth shot at 390 kV.

The O-ring groove edges were machined to a 0.015-inch radius and a straight edge Lucite envelope similar to No. 4 was tested as No. 8. Some flashing occurred at 294 kV but conditioning occurred up to 364 kV. The voltage was lowered to 332 kV

where the insulator held and then pushed up to 342 kV where oil surface tracking occurred. It is believed that this was due to oil impurities settling out on the insulator surface. After cleaning, the insulator held 378 kV for 44 shots before again failing at the O-ring groove edge.

Insulator No. 9 (Figure A-2f) was an attempt to preserve the usefulness of the gradient-ring-mechanical-stop concept, as well as to evaluate the effect of letting the gas glow at the O-ring groove edge by maintaining air at atmospheric pressure. In this case the unit was assembled without evacuation or pressurization. It was speculated that the discharge (if any) might diffuse and reduce the fields. The oil side was machined with a concave radius section 0.20-inch deep with a 0.030-inch edge which fitted against the aluminum step. The intent was to reduce the surface component of the field in the oil at the triple junction. Failure occurred at 417 kV. The mode appeared to be volume puncture at both sides and surface tracking between breakthrough points on the oil-Lucite surface.

Insulator No. 10 was a straight Lucite ring coated on both sides with conductive silver paint. Flashing occurred at 240 kV and 10 of 10 shots at 267 kV flashed. In coating the surfaces some paint got on the inner surface but was cleaned by polishing. The thickness of paint could not be carefully controlled and examination of the ring after shooting disclosed that tracking continued around the corner of the Lucite suggesting there was at least a small separation of Lucite and aluminum.

The general conclusion was that within the limits of these tests, the straight edged envelope was as good or better than the other shapes, and that the upper limits in any operating switch might be breakdown right through the oil or volume breakdown from "O"-ring grooves. Lexan was rejected due to its continued degradation after flashing, i.e., the weak spot became continually weaker.

A.2.2 SEGMENTED ENVELOPE TESTS

Based on the results of the single stage tests, a segmented envelope was constructed as shown in Figure A-8. Major differences in design were the shape of the gradient rings and the O-ring grooves. The gradient rings are 0.125 inch thick and the O-ring grooves are 0.140 inch wide by 0.077 inch deep compared to 0.344 inch wide by 0.205 inch deep for the test fixture electrodes. Additionally, the insulator diameters were shrunk from 10 inches to 8 inches inside diameter and 12 inches to 10 inches outside diameter in order to reduce the overall size.

A basic schematic of the test system is given in Figure A-9. The Marx generator and test tank are the same as used in the oil switch experiment. The oil capacitor is used to smooth the Marx generator output waveform. It consists of the trigger Blumlein line components from the oil switch tests. The dump gap was a point plane, self-breaking oil switch. Originally mounted with the point negative, it was later modified with point positive to get better breakdown characteristics. R_1 was eliminated during testing in order to get sufficient voltage output, i.e., increase the Marx gain. R_2 was on the order of 60 ohms and served to both smooth the waveform and damp the Marx discharge following dump gas closure. R_3 started as 1200 ohms but was later reduced to 300 ohms, again to produce a greater percent of Marx output voltage across the switch. R_3 and the switch monitor formed a voltage divider through which the capacitance of the switch is charged.

At the start of testing, the envelope was assembled with 12 stages without the stainless-steel electrodes and then was mounted horizontally in the tank. Prior to filling the tank with oil, the switch was evacuated and backfilled with SF_6 gas directly from a bottle, the same one used in single insulator tests. Pressure was maintained by means of a regulator.

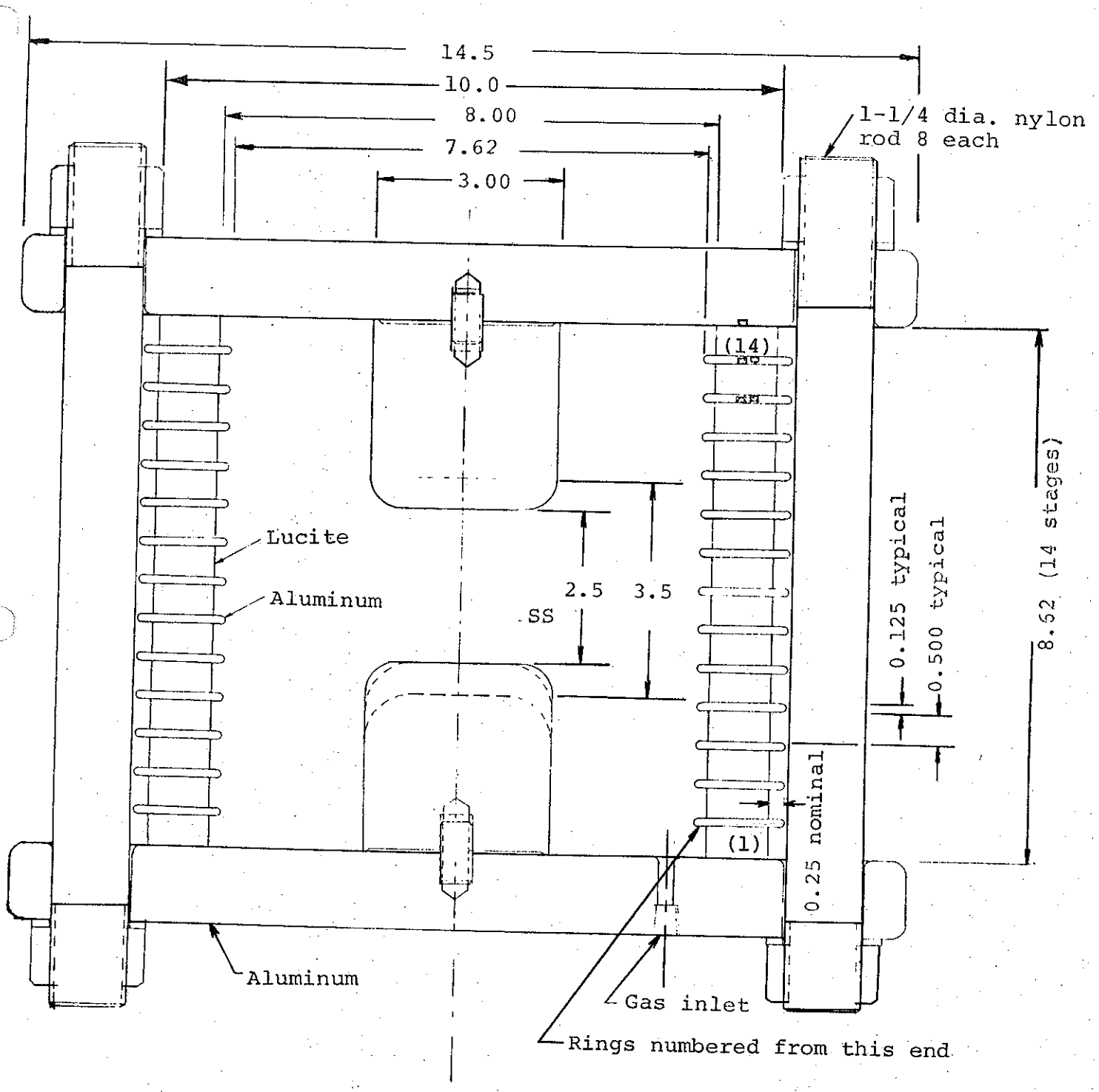

Note: All dimensions shown are in inches.

Figure A-8 Segmented envelope structure.

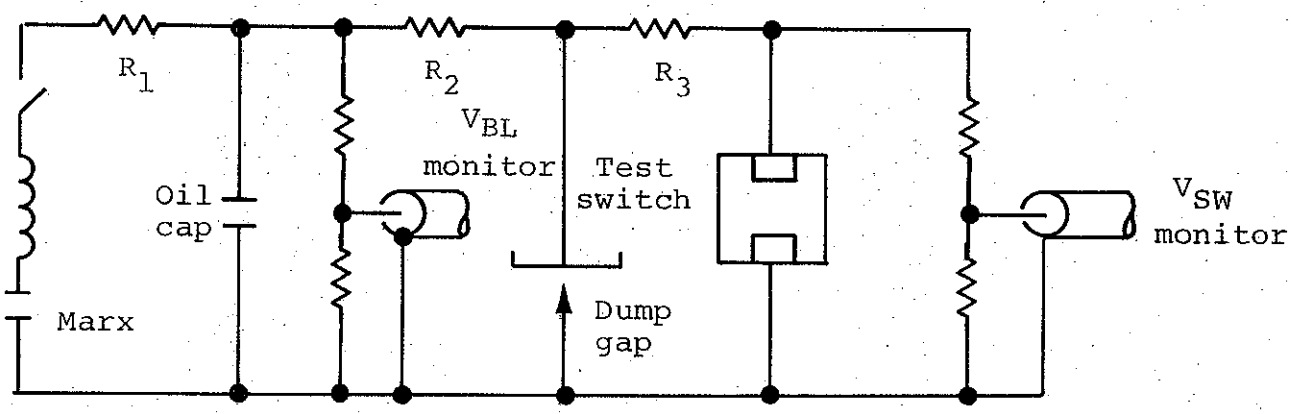

L_M = 18 μH
C_M = 12 nF

Figure A-9 Basic schematic of segmented envelope test system.

The charging waveform was determined by the circuit constants, and the amplitude (and hence duration) of voltage applied to the switch envelope was controlled by the Marx charge voltage and the spacing of the dump gap. To change voltage over small intervals either charge voltage or spacing could be changed, but in order to preserve time to dump gap breakover, it was necessary to vary both.

Starting with 120 psig SF_6 in the switch, 1.5 MV peak was applied on the first shots. The voltage was raised in several steps until at 2.4 MV the envelope flashed over with both visual and monitor trace confirmation, with similar results at 2.2, 2.5 and 2.3 MV. After holding at 1.6 and 1.3 MV, the switch failed at 2.23 MV in an oil arc. Initial observations of the switch in the tank showed tracking had occurred along one of the top nylon tie rods and the switch was removed to the bench for closer study. The tracking began near the negative end and followed surface flaws (lengthwise scratches) in the rod. Surface tracks were found both on the oil side (3) and gas side of the insulator rings and the switch was dismantled for thorough examination of the track marks. Table A-2 is a listing of the location of the internal tracks at the gas-insulator surface. The circumferential location is the space between nylon rods as viewed counterclockwise from the ground end. The rings are numbered sequentially starting at the ground end. The three oil-insulator surface tracks were on the uppermost part of the rings where impurities are most likely to settle. In all three cases, the tracks branched in both directions with a missing portion of track near the start.

Prior to reassembly and continuation of testing, the insulator rings were remachined on the inner surface to remove all traces of track marks. The gradient rings were hand polished to remove the damage due to the arcs. The nylon rods were carefully cleaned and, in subsequent tests, the switch was washed with oil if debris was observed to be settling on the rings during immersion in oil.

TABLE A-2: Location of tracks on insulator rings following tracking of nylon rod. Number 1 ring is the ground (plus) end of stack.

	CIRCUMFERENTIAL LOCATION							
	BOTTOM							TOP
Ring No.	1	2	3	4	5	6	7	8
1	2		2					
2		1		1	2			
3	1	1	1	2	2	1	(OIL)	
4	1	1	1	2				1
5			1	2	2			(OIL)
6			1		2			
7			1	1				
8		1	1	4	1			
9			1	4	3			(OIL)
10		1		1	1			
11			1	1	1	1		
12				1	2	1		

The switch was pulsed approximately 125 times at voltages ranging from 1.5 to 3 MV during which the pressure was maintained at 120 psig. When the envelope flashed at 2.94 MV, the switch was again disassembled for inspection. The track mark locations are given in Table A-3.

The rings were again machined on the inner diameter to remove track marks and the gradient rings were hand worked before being reassembled with two additional rings making a total of fourteen. The switch was mounted with its axis vertical, the ground (plus) end being on the top. In addition two field shaping electrodes were added in order to make the voltage division among the rings more uniform. The ground end electrode was 3 feet in diameter with a radius of about 0.5 inch to a skirt. The high voltage end field shaper was approximately 34 inches in diameter and consisted of a sheet of plywood covered with aluminum foil to give a good optical reflecting surface. The pressure was raised to 150 psig.

The switch then withstood almost 4 MV successfully. The peak switch voltage for the succeeding series of shots is plotted in Figure A-10. Shots 34 and 35 may have had some insulators flash but the stack held voltage as shown in Figure A-11a. A trace showing gas switch flashing is given for comparison in Figure A-11b. No other visual indication of flashing was observed nor did any scope trace indicate breakover. At values of 183 and 170 kV/cm, individual insulators may have flashed but the envelope held. Typically the envelope was stressed to a value of 180 kV/cm at 150 psig SF_6 and 200 to 220 kV/cm at 175 psig SF_6 without flashover. The pressure was raised to 175 psig following shot No. 37.

Having determined a lower bound ($\sim$ 3.5 MV) of insulator holdoff voltage, the next step was to develop electrodes compatible with the required switch inductance and self-break voltage and to determine, if possible, the effect of electrodes on envelope flashover.

TABLE A-3: Location of tracks on insulator rings on second unstacking inspection.

Ring No.	Number of Tracks	Location	Branching
1	6	Lower half	From +
2	3	Bottom	2+, 1 Unbranched
3	16	12 on bottom	10+, 2-, 4?
4	5	--	3 Both directions
5	5	4 Bottom, 1 TDC	3+, 2 Both
6	3	Bottom	+
7	2	1 Top 1 Bottom	+
8	2	--	+
9	1	Bottom	+
10	1	Bottom	+
11	4	Bottom	3+, 1 Both
12	4	Bottom	3+, 1 Unbranched

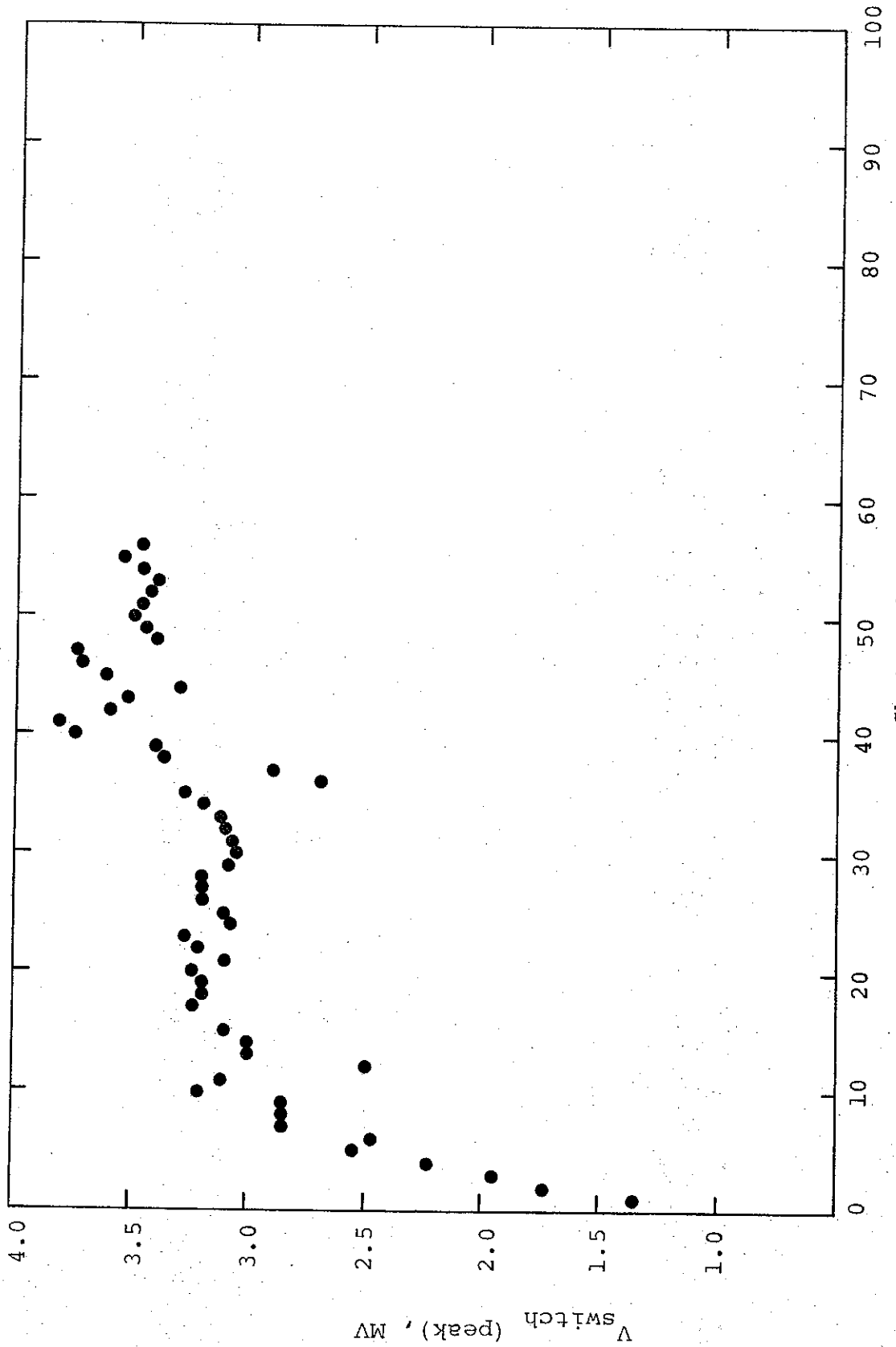

Figure A-10 Peak voltages applied to 14-stage segmented envelope of gas switch without electrodes.

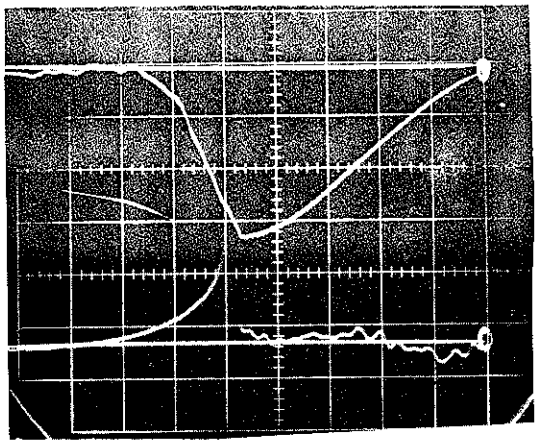

Upper traces: V_{switch}

Vertical: 1.0 MV/div

Horizontal: 100 nsec/div

(a)

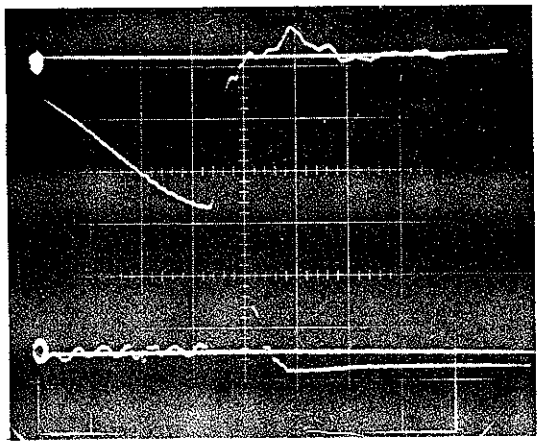

(b)

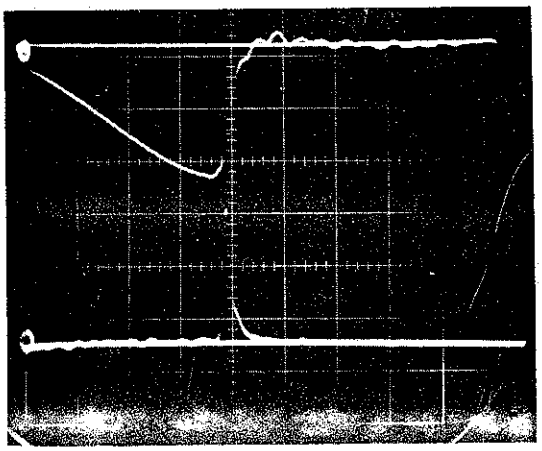

(c)

Figure A-11 Comparison of shot records for dump gap only closing (a), switch flashover (b), and dump gap closing with switch flashover following (c).

Electrodes were installed as shown by the solid lines of Figure A-8 which gave an electrode spacing of 2.5 inches. All shots with these electrodes are plotted in Figure A-12. Breakover occurred on shot No. 3 at 2.85 MV. The trace for this shot is given in Figure A-11b. The voltage was then lowered in steps until at 2.52 MV the switch flashover occurred after the dump gap had already closed. The switch held at 2.1 MV at shot No. 7.

The switch was removed to the bench for examination of the electrodes. All arcing had occurred near the tangent point on the ends in a length of about 1 inch. The electrode radius was increased to 0.75 inch and the end tangent point was blended to feel smooth.

Several insulators flashed on the first succeeding shot (No. 8) without total breakover, and again at 2.84 and 3.04 MV. None were observed at 3.33 MV, but the switch closed at 2.90 MV and 2.6 MV. The only damage that could be seen with the switch in place was a track on each of insulators Nos. 2 and 3.

Following shot 26, the switch was removed to a bench where in addition to the tracks on 2 and 3, a single track on No. 1 and 12 rings and multiple tracks (grouped over about a half inch) on No. 14 were found. Only the tracks on 2 and 3 were aligned.

One endplate was removed for examination of the electrodes and inner surfaces of the rings. The arc marks on the electrodes were concentrated over approximately one fourth of the circumference and loosely grouped about the tangent of the end to the corner radius. The electrodes were buffed to remove all arc marks.

Before the electrodes and endplate were replaced, the inner exposed surfaces of the insulator and gradient rings were cleaned with lint-free wipes in the stacked condition, i.e., no unstacking or track cleanup was made.

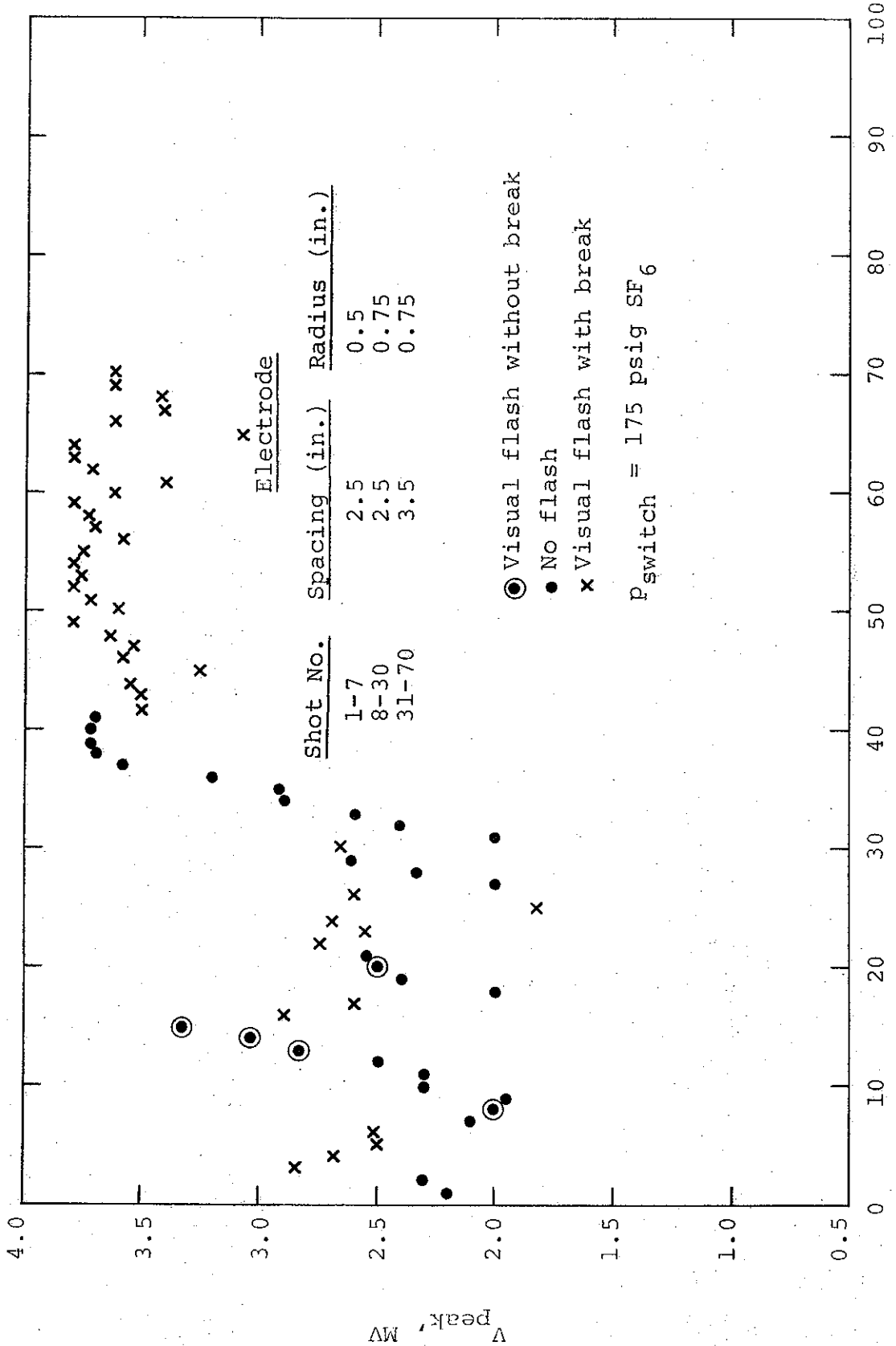

Figure A-12 Voltage data of 14-stage segmented envelope gas switch with three inch diameter symmetrical electrodes. (See Fig. A-8).

On the fourth shot (No. 30) following restart of testing, the switch flashed at 2.65 MV. The switch was again removed to the bench to check the breakdown mode. A single arc mark was found on each electrode. These were symmetrically opposite each other and located approximately 1/4-inch inside the tangent circle on the end.

In order to increase the electrode dominated self-break of the switch, the electrode spacing was increased from 2.5 inches to 3.5 inches by removing 1/2-inch from the base of each. The faces were buffed to remove the arc marks and the electrodes and end plate replaced. The insulator gradient ring inner surfaces were wiped to remove lint.

Again the switch was mounted in the tank and testing continued as the voltage was raised in steps to 3.72 MV without flashing so the pressure was lowered first to 165 psig on shot 40 which held 3.70 MV, and then to 150 psig on shot 41 with breakdown at 3.50 MV. The pressure was increased again to 175 psig and pulsing continued. On shot 56 the dump gap went to 3.58 MV with the switch breaking over approximately 40 nsec later at 3.0 MV. (See Figure A-11c.) On shot 60 a small insulator flash was observed but the switch held when the dump gap fired at 3.61 MV. There was no indicated reason for the low value (3.08 MV) for shot 65.

At the end of the series, arc marks were found to be rather uniformly distributed over both electrodes over the radiused section.

Increasing the holdoff of the insulator stack would allow either shortening the overall switch for lowered inductance and cost for a given voltage holdoff, or for a given switch operation

could be at a reduced percentage of self-fire voltage for increased reliability. As the number of switches increase, the latter becomes increasing important. Possibility of such increase is strongly suggested by comparison on the single to stacked insulator flashover fields, and consideration of a static field plot of an envelope with electrodes.

First breakover of the single straight edge insulators was observed at 206 kV/cm (No. 1), 185 kV/cm (No. 2), 195 kV/cm (No. 8) and 315 kV/cm (No. 4) at 120 psig SF_6. Number 4 was, however, a retest of No. 2 with one internal trackmark polished out so that a value of around 200 kV/cm would seem (on a statistically very small sample) to be the typical fresh insulator flashover. The initial flashover strength of both the 12 (120 psig) and 14 (150 psig) insulator stacks was 185 kV/cm neglecting field enhancement. That is, this value is the total voltage divided by a product of the number of rings and the single insulator length (1.27 cm). This would seem to indicate that the stacked and single insulator flashover field strengths might be comparable.

Single insulator test results indicated that the conditioned strength of a single insulator on the gas side was in excess of 300 kV/cm, the field at which breakdown at the O-ring groove tended to occur. On test No. 4, a value nearer 350 kV was measured prior to failure at the O-ring at 365 kV/cm.

A field plot of this switch configuration was prepared by Sandia Laboratories for the switch installed in a closed coaxial line. This plot is reproduced in Figure A-13. An estimate of uniformity of field was made from this plot by estimating the potential on the gradient rings from this plot and plotting

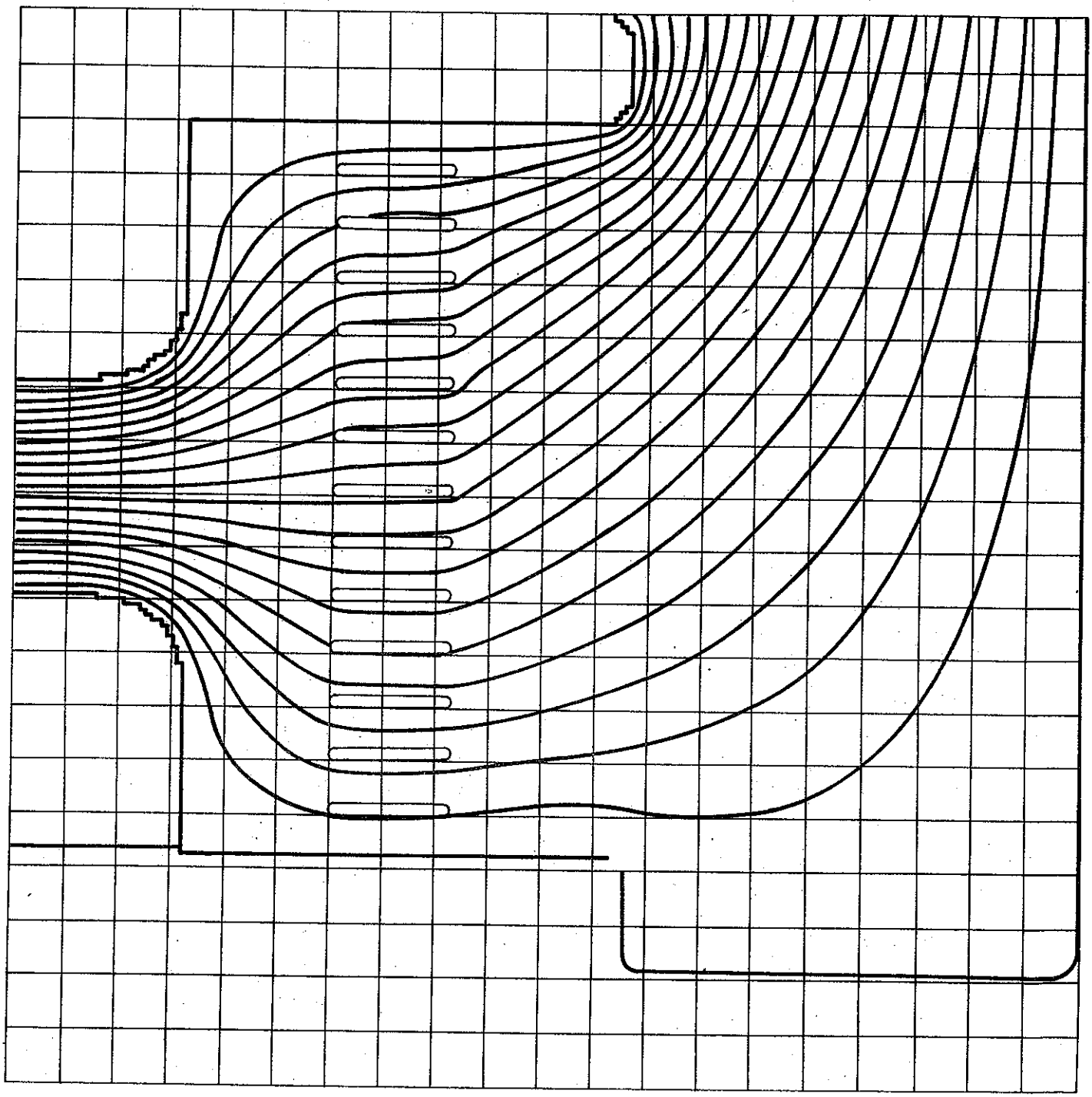

Figure A-13. Field plot prepared by Sandia Laboratories for the 14-stage simulator stack with electrodes. Field lines of 5 percent are plotted on a 1/2-inch grid.

SECTION A-3

TRIGGERED GAS SWITCH TESTING--PHASE II

The gas multistage segmented insulator switch was modified as shown in Figure A-14 to include a trigger electrode and TIG with provision to individually control the pressure of the main chamber and the TIG. The diameter of the electrodes was increased from 3 inches to 4 inches, the edge radii increased to 1 inch, and the sparking area was made of brass. The trigger electrode was made of SS303. The major diameter of the electrode disk was 2.75 inches. It doubly tapered from a thickness of 0.030 inch to a sharp edge over a distance of 0.060 inch. The trigger electrode stickout (TESO) was made adjustable by removing the center of the TIG electrode and inserting a wrench through the center of this electrode and engaging a captive 6-40 set screw in the trigger electrode.

Inclusion of a trigger isolation gap in the switch allows a wide range of trigger source design. The requirements to be met are that the TIG isolates the trigger electrode allowing it to capacitively float to the desired potential corresponding to its geometry and spacing from the near electrode (trigger electrode stickout) and that the trigger pulse be of sufficient amplitude to cause rapid overvoltage of the TIG when combined with the existing trigger pulse charge voltage which appears on the TIG. In the event the trigger source is at ground potential, the TIG must hold off full trigger electrode voltage. This was assumed to be the worst case for TIG holdoff, and hence switch

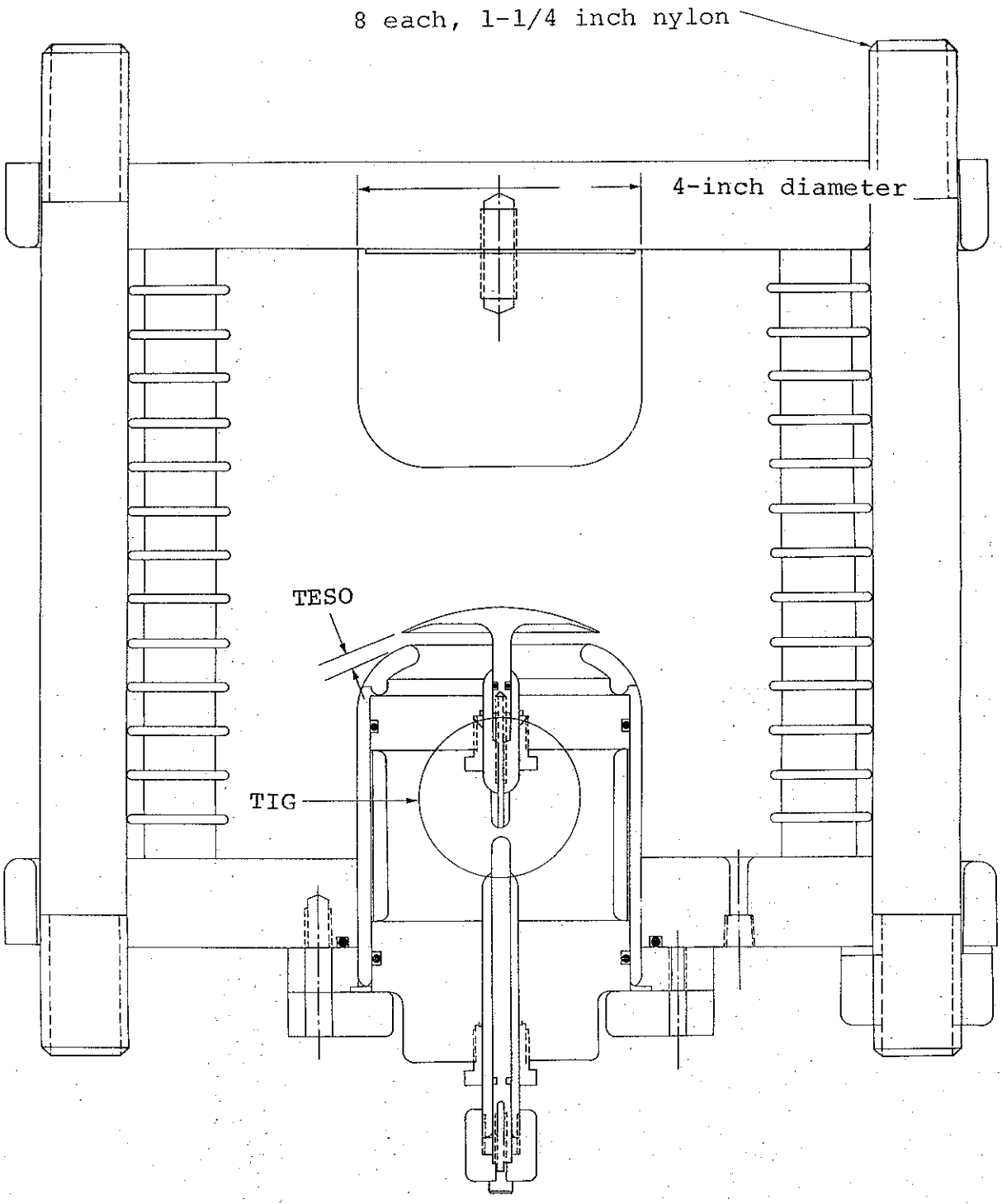

Figure A-14 Partial assembly drawing of triggered gas switch.

tests were made with the TIG source electrode grounded. In triggered tests, the trigger voltage was derived as an integrated fraction of the charging waveform so that the voltage on the TIG was greatly reduced during pulse charge in comparison to these tests.

The self-break value of the switch as a function of TESO was measured starting with an electrode spacing (TESO=0) of 2.5 and 3.0 inches with the same test circuit used in the multistage segmented insulator tests. Switch pressure was 175 psig SF_6 in these tests.

The data for main electrode spacing of 2.5 inches are plotted in Figure A-15. This spacing (rather than the 3.5 inches of the envelope tests) was chosen to provide an initial curve at less than peak envelope test voltages but with the expectation of some increase in self-break values due to the increased diameter and edge radii of the electrodes. Balance (maximum holdoff) was found for a TESO of 0.25 inch or n = 10 although electrically it might be less, say n = 8, due to field enhancement. During tests it was necessary to increase the TIG spacing from 0.25 to 0.44 inch in order to prevent TIG closure with a grounded TIG electrode.

The switch was disassembled and cleaned before reassembling with an increased electrode spacing to raise the self-fire voltage. Inspection of the electrodes disclosed five heavy arc marks on the negative (solid) electrode and many fine arc marks. The trigger electrode had five arc marks on the surface approximately 1/2 to 3/4 inch away from the edge but scattered and many marks around the periphery of the sharpened edge. The arcs on the near electrode were well distributed. Multiple tracks were found on insulator No. 1, and single tracks on insulator Nos. 2, 12, 13,

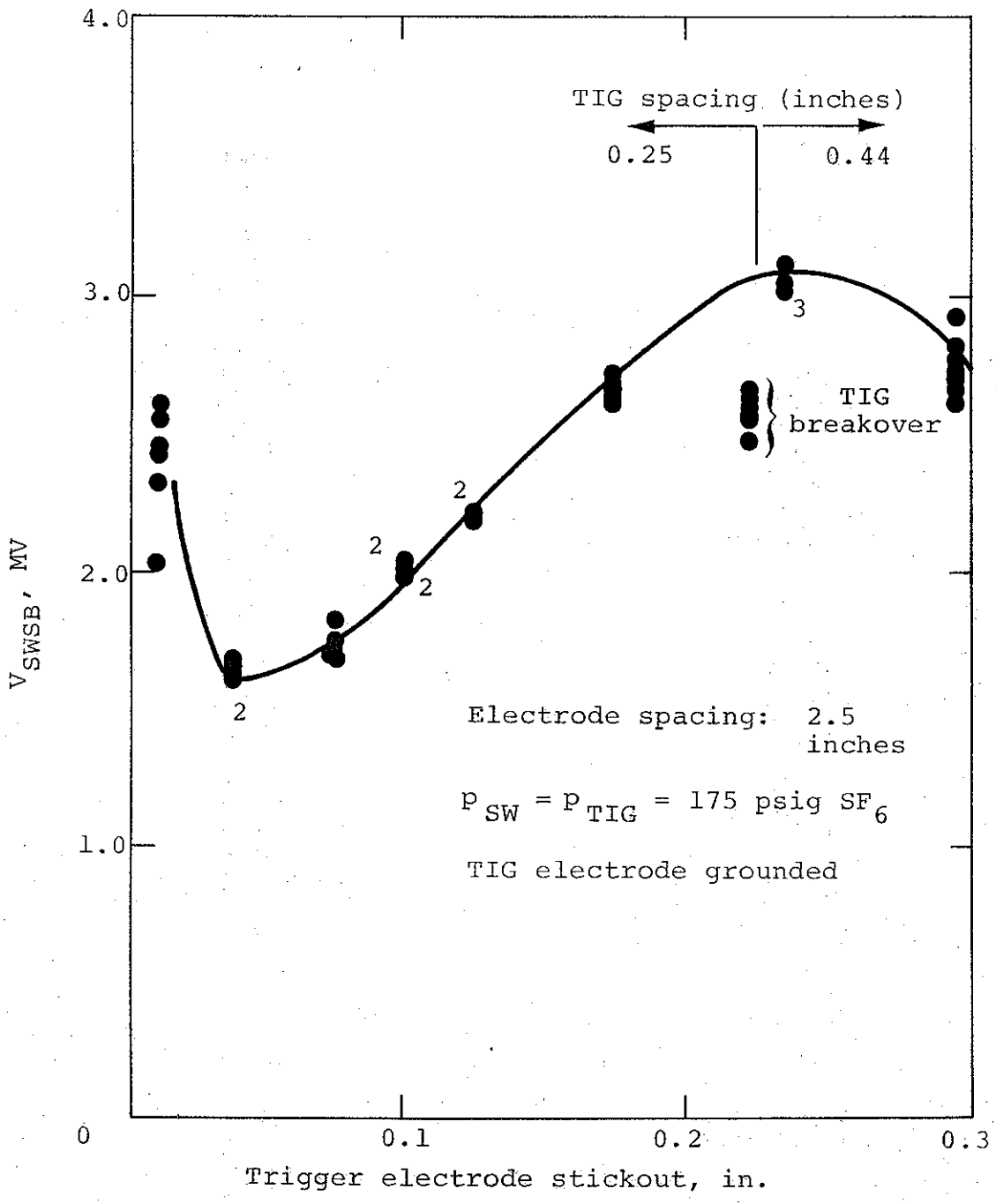

Figure A-15 Switch voltage self-break valves for an electrode spacing of 2.5 inches and various trigger electrode stickout. (Multiple data points indicated by number.)

and 14. Only insulator No. 13 had not previously been noted as tracked. No cleanup of tracks was made except for wiping with Freon TF.

The electrode spacing was increased to 3.0 inches by removing 0.25 inch from the solid electrode, and adding a 0.25-inch spacer between the flange of the trigger end electrode and endplate. Data for this spacing is shown in Figure A-16. Again, TIG breakdown required an increase in TIG spacing. At a TESO of 0.25 inch the self-break values showed a large scatter so the switch was dismantled for inspection. Two additional tracks were found on insulator No. 14 but were not judged to be serious enough to cause the data scatter or breakdown. The insulator and gradient rings were wiped with lint free wipes to remove any haze or dust. Then, just prior to installing the trigger electrode assembly, the opposite solid (fixed) electrode was found to be loose and away from the endplate approximately 1/4 inch. A possibility exists that some of this spacing may have been caused by rotating the electrode during wipe down of the insulators but an immediate review of the procedure at the time suggested it was not likely.

All insulators and rings were cleaned with dry, lint-free wipes to remove most of the surface haze and the switch was installed for continued testing at TESO of 0.3 inch.

Next at TESO of 0.26 inch self-break values were again scattered and low. The acrylic plate supporting the trigger electrode was found to have multiply tracked through. The arc appeared to start at the threads nearest the small O-ring. This part was replaced and more data points taken at TESO = 0.25 inch and a TIG spacing of 0.71 inch. A self-break value of $V_{SWSB} \geq 3.3$ MV was determined.

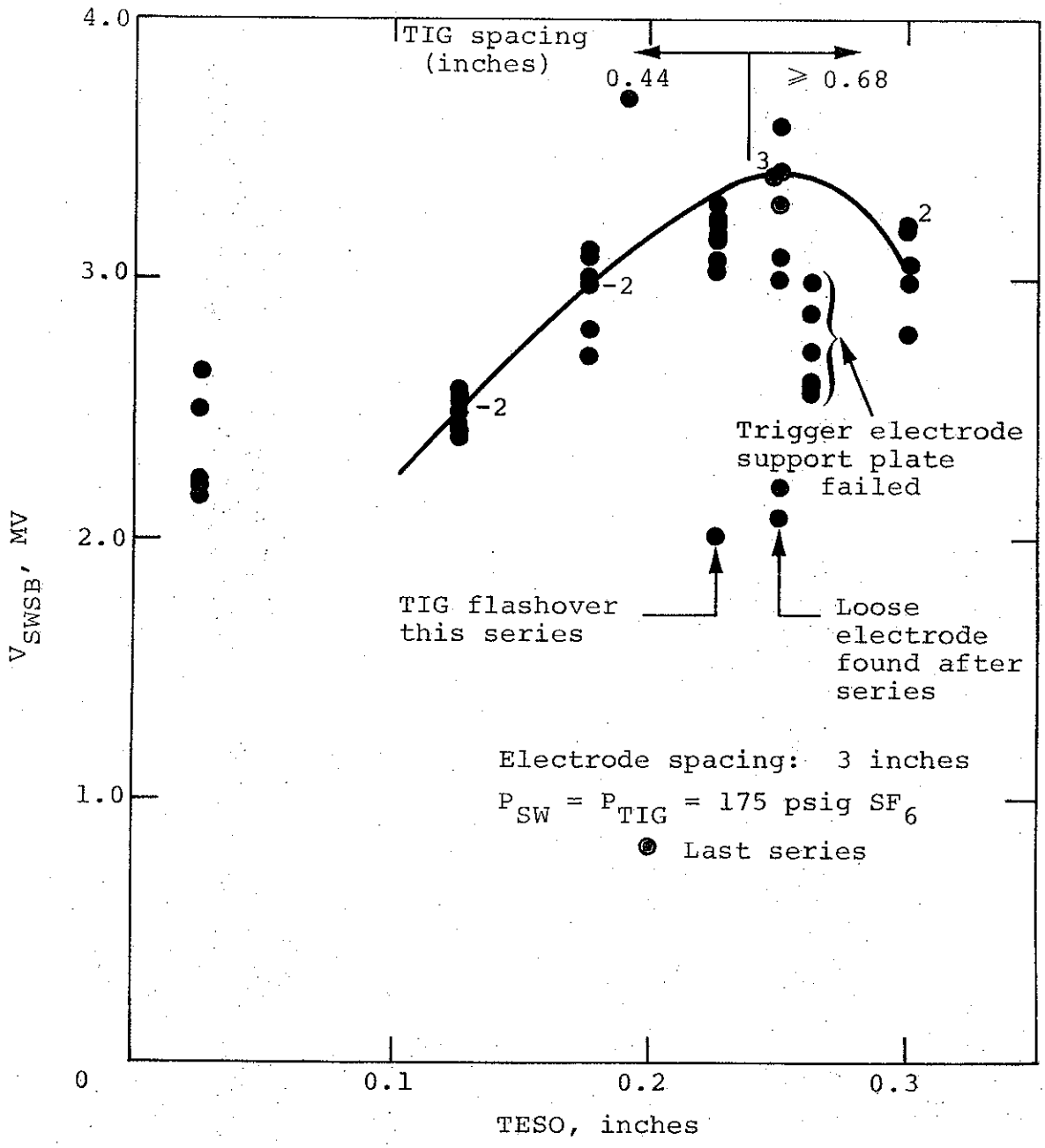

Figure A-16 Switch voltage self-break data for an electrode spacing of 3.0 inches and various trigger electrode stickout. (Multiple data points indicated by number.)

The test setup was next modified to provide a trigger pulse. A basic schematic is given in Figure A-17. C_{SW} represents the capacitance of the switch and field shapers. R_4 was initially infinite. The oil capacitor is the oil transmission line initially used to provide a trigger in the oil switch tests and smooths the output of the Marx generator. R_2 is approximately 60 ohms and is a sink for the dump gap. R_3 is 300 ohms and limits the current through the test switch so that the dump gap will fire. The TIG series resistor started at 20 ohms.

The trigger cable is a length of high voltage coaxial cable pulse charged to some fraction of the switch voltage as determined by the ratio of R_1 to the monitor resistance of the self-breaking trigger cable gap (V_{CSG}) and the capacitance of the trigger cable. With closure of the cable shorting gap, a pulse is sent down the trigger cable. This pulse overvolts the TIG through the series limiting resistor, and then drives the trigger electrode in the opposite polarity to the pulse charge value, thus initiating switch closure.

Initial tests involved varying values of R_1, V_{CSG} monitor resistance values, CSG spacing and pressure, and TIG spacing until the conditions for triggered switching were achieved. RG-220/4 was used for the initial trigger pulse cable. This failed eventually after having been subjected to voltages in excess of 350 kV and was replaced. The replacement RG-220/u cable failed at lower pulsed charged voltages. A section of Belden YR-13181 was substituted and no further trigger cable problems were encountered. In Figure A-18 typical waveforms are shown of a series of shots for which p_{SW}, P_{TIG} and p_{CSG} are respectively 120, 70, and 34 psig SF_6, and the dc charge voltage of the Marx is 70 kV. The switch and trigger line voltage waveforms are straightforward. The lower waveform is

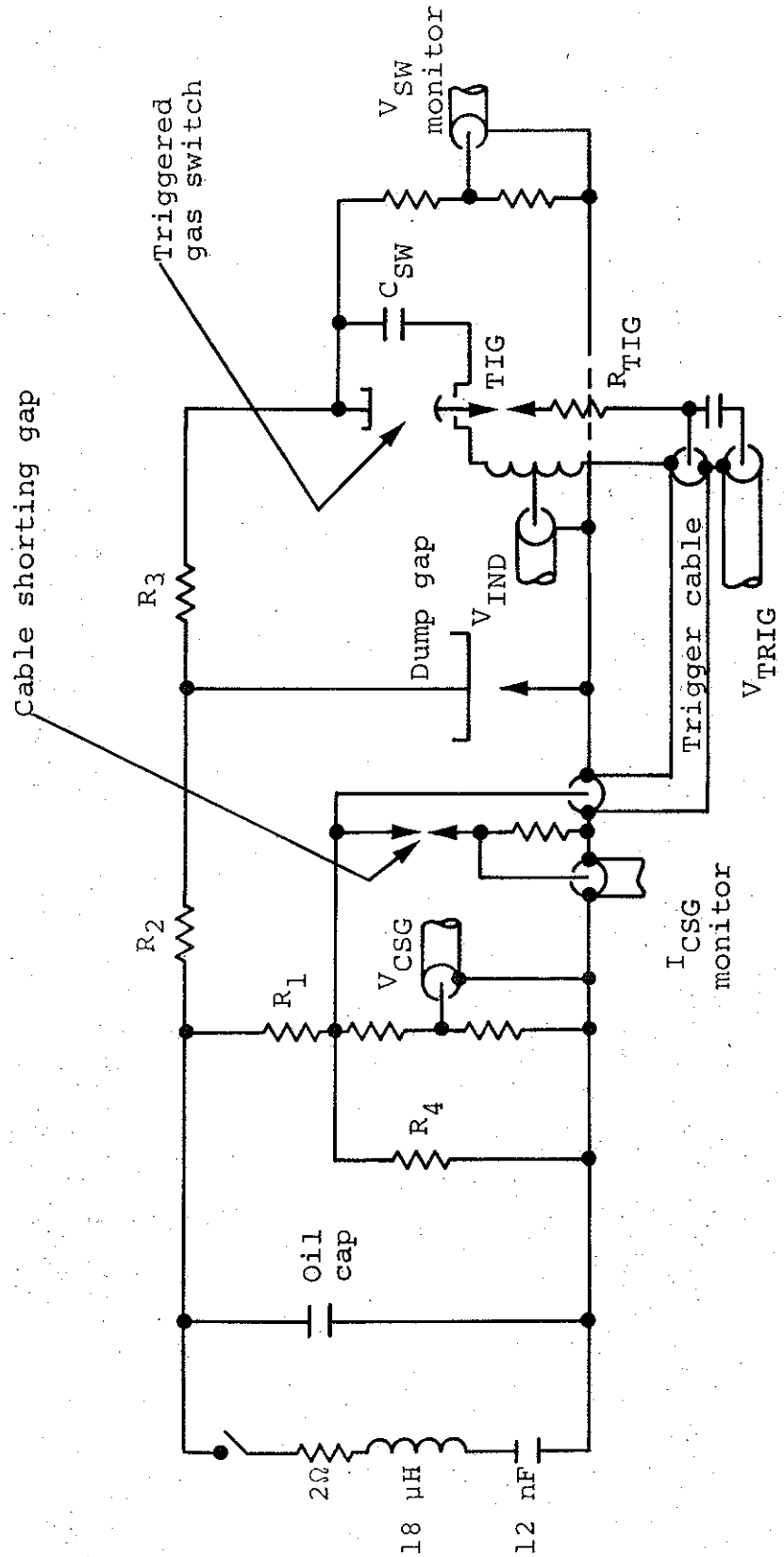

Figure A-17 Basic schematic of oil tank layout for triggered gas switch tests.

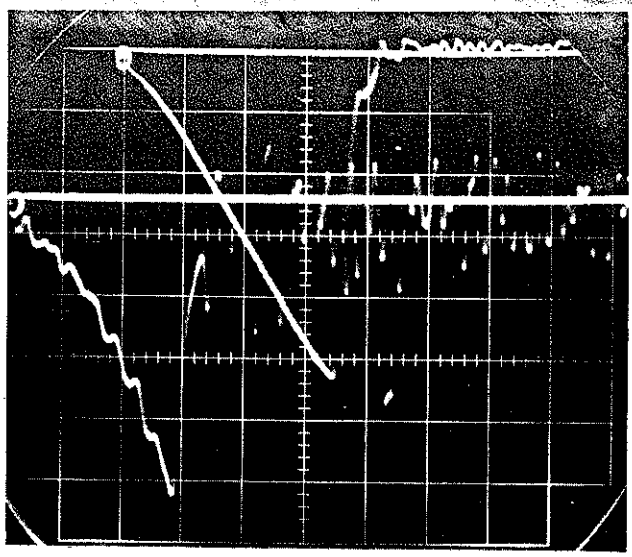

Top: V_{SW}

Vert. Defl: 0.5 MV/div

Horiz. Defl: 100 nsec/div

Bottom: V_{CSG} (trigger line voltage)

Vert. Defl: 50 kV/div

Horiz. Defl: 100 nsec/div

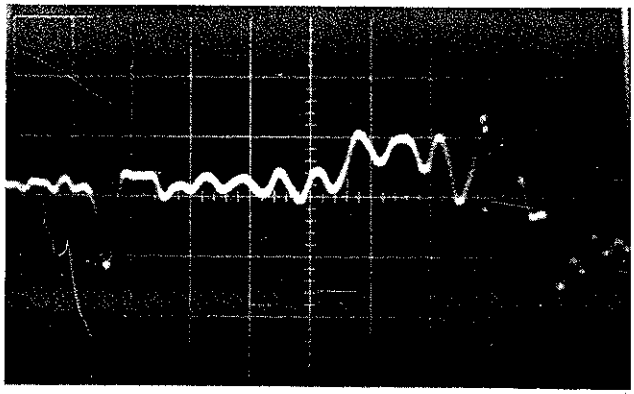

$I_{CSG} + V_{TRIG} + V_{IND}$

Horiz. Defl: 10 nsec/div

Figure A-18 Typical oscilloscope traces from which data plotted in Figure A-19 are derived.

the sum of the output of three monitors. The signal from the resistor in series with the trigger cable shorting gap is used to trigger the oscilloscope externally and is then displayed internally on Channel B. This appears as a negative going signal approximately 14 nsec into the grid. The signal obtained from a capacitive pickup at the output end of the trigger cable is mixed with the delayed signal obtained from an inductive division of the switch voltage appearing on the chain supporting the switch in the oil tank. The former appears as a positive going signal 55 nsec into the grid and the latter causes a sharp negative break at 79 nsec.

A direct comparison of traces from individual monitors combined with cable length measurements were used to assure the correct interpretation of events. For this presentation a fixed delay equal to the pulse length of the trigger line occurred between the I_{CSG} and V_{TRIG} signals since the cable lengths from the monitors had been adjusted to be equal with 1 nsec. The data available from this series concerns the switch voltage, trigger voltage, and switch closure time, and are 2.61 MV, 240 kV, and 24 nsec, respectively for the traces of Figure A-18. Times are estimated to within 1/2 nsec with probable accuracy within 1 nsec.

The integrating effect of the trigger cable charging circuit is clearly seen by comparing the shapes of the waveforms in the upper photograph.

Data from a series of shots are plotted in Figure A-19. Self-break was not measured at 120 psig, but a linear interpolation from 175 psig would give a value of 2.4 MV for self-break. Since no self-breaks were observed in this series, it must be assumed that self-break is not exactly linear with pressure.

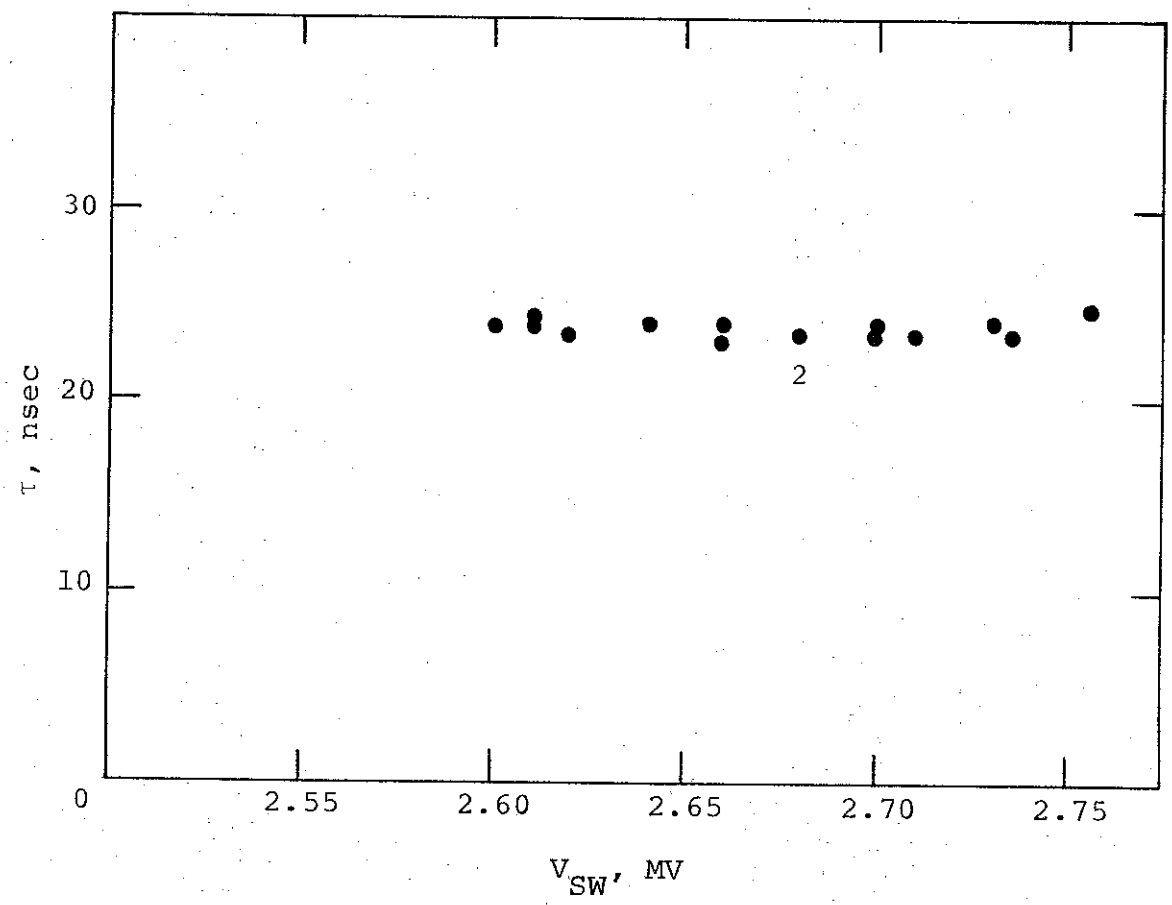

Figure A-19 Triggered closure times for switch voltages near peak of the changing waveform.

In order to assess the effect of the TIG pressure on closure times, a series of shots were made with all parameters fixed except for TIG pressure. The data of Figure A-20 gives the results, a nearly linear increase with pressure. During this series the switch voltage varied from a maximum of 3.11 MV to a minimum of 2.88 MV. The TIG pressure was then held constant at 45 psig and the CSG pressure varied to change the voltage over the range 3.1 MV to 2.72 MV. These points are included in Figure A-20.

Changes following this series included improving the capacitive pickup on the trigger output monitor, installation of a dryer in the switch gas line, increasing the series TIG resistance from 20 ohms to 50 ohms, and installation of the high-voltage trigger line coax cable.

Closure time and jitter measurements were again made but at pressures of 150 and 175 psig SF_6 from waveform data shown typically in Figure A-21. The trigger monitor output was separated from the I_{CSG} and V_{IND} outputs and displayed separately on a 5 nsec/div display. This monitor shows the arrival of the positive trigger pulse (near trace start), the negative break at TIG closure (2.4 divisions), and end of trace at 5 divisions when a negative signal due to switch closure is induced in the monitor. Time of switch closure is plotted in the upper portion of the Figure A-22. Total switch closure times were read from the 10 nsec/div trace of Figure A-21 and are plotted in the lower portion of Figure A-22. A fixed delay of 18 nsec is included in these latter data.

The switch closure time following TIG closure was measured with a probable error less than 0.2 nsec. The absolute time spread was 10.3 to 14.5 nsec averaging about 13 nsec with a jitter of 0.9 nsec.

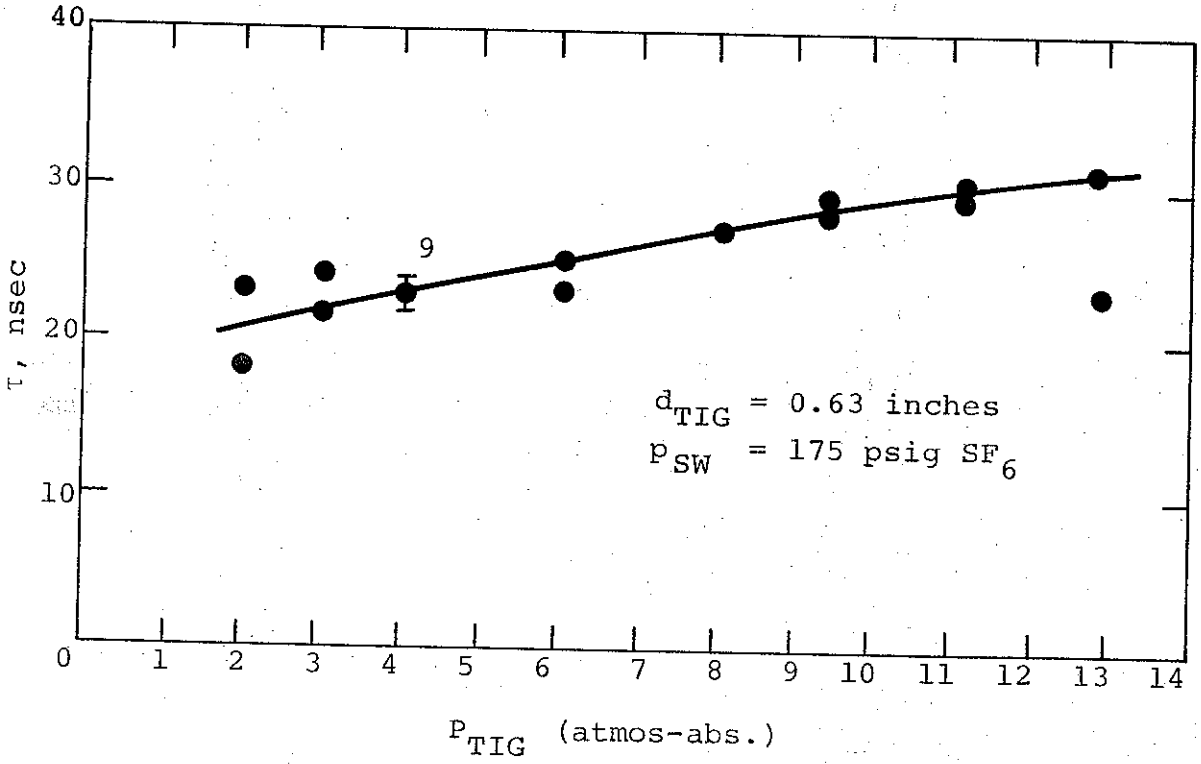

Figure A-20 Switch closure time for variable TIG pressure.

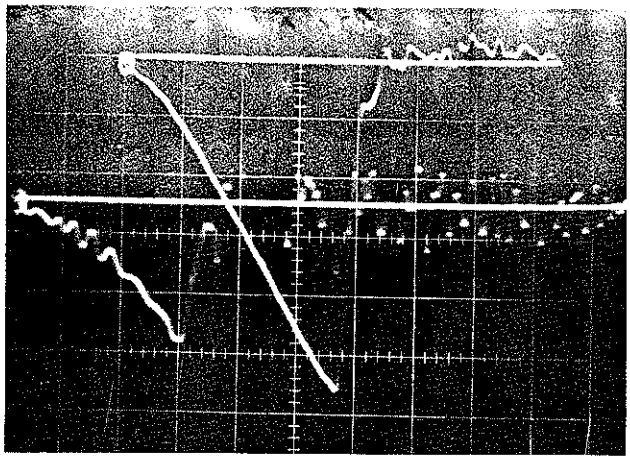

Top: V_{SW}

Vert. Sens: 0.5 MV/div

Horiz. Sens: 100 nsec/div

Bottom: V_{CSG}

Vert. Sens: 100 kV/div

Horiz. Sens: 100 nsec/div

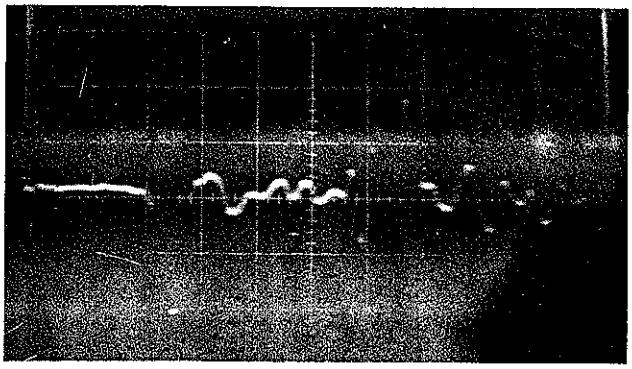

$I_{CSG} + V_{IND}$

Horiz. Sens: 10 nsec/div

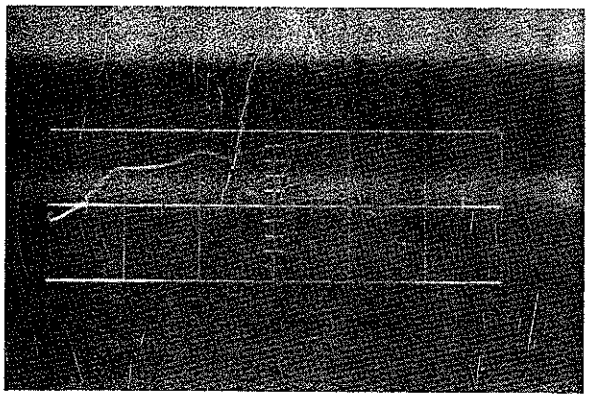

V_{TRIG}

Horiz. Sens: 5 nsec/div

Figure A-21 Typical oscilloscope traces from which timing data are derived.

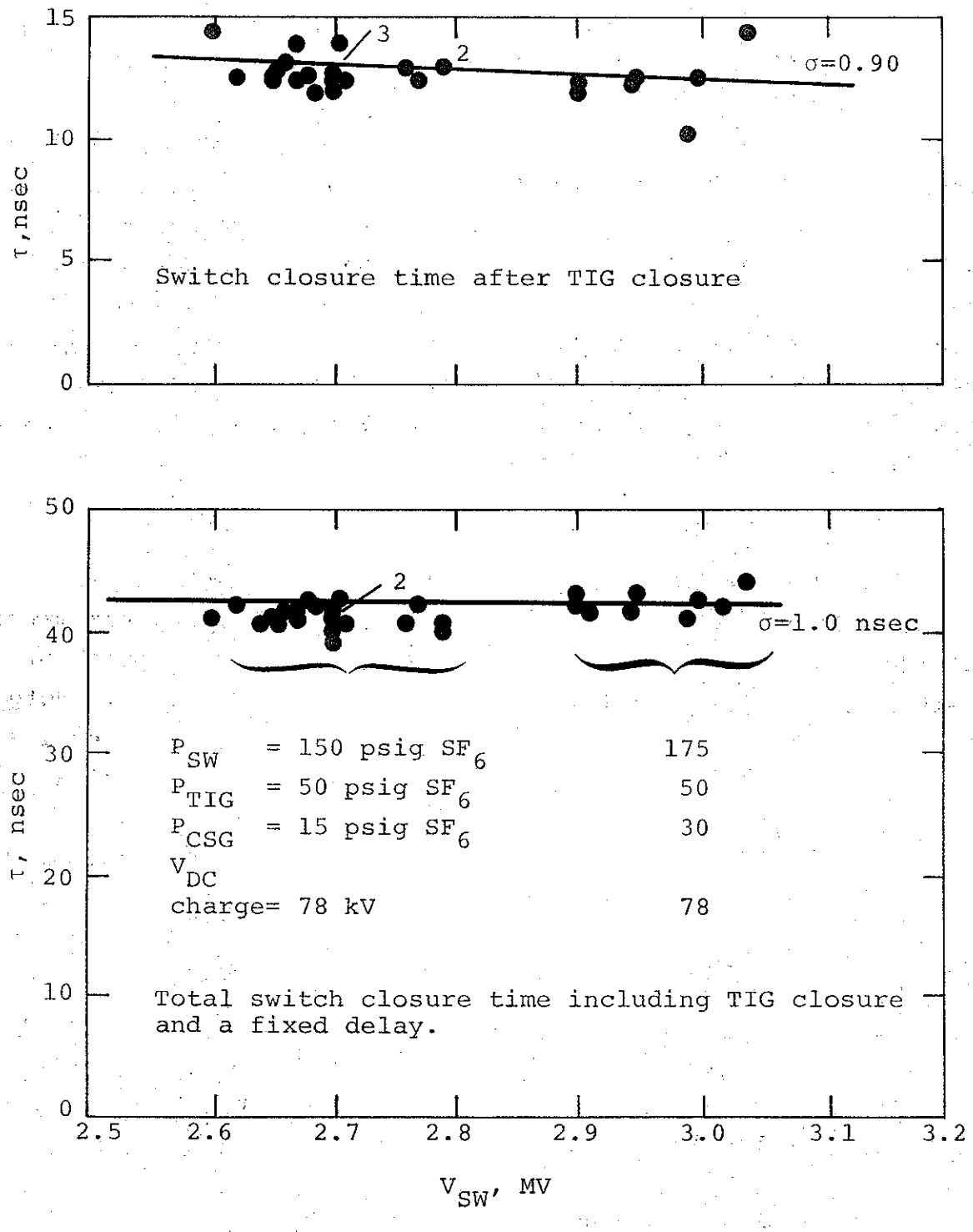

Figure A-22 Closure time and jitter measurements with improved monitoring.

TIG closure was measured directly from the V_{TRIG} monitor trace and as the difference between switch closure from this trace and the total time measured from the I_{CSG} and V_{IND} monitor output. Reading error from the V_{TRIG} monitor was introduced by the uncertainty of trigger pulse start due to finite risetime. Reading accuracy from the 10 nsec/div trace was better than 0.5 nsec/div however and comparison of a number of traces suggested that probable error in reading overall time from either trace would be less than 0.5 nsec. Total closure time averaged 24 nsec with a measured jitter of 1.0 nsec. TIG closure was measured as the difference or 11.5 nsec. A quadrature summation of jitter times would assign a value of 0.95 nsec to TIG closure jitter.

The switch was next moved to the side of the tank and connected directly to an oil transmission line of approximately 60 ohms impedance and 20 nsec pulse length. A photograph of the switch in position in the tank is shown as Figure A-23. Note that the switch has been remounted with the axis horizontal and the end field shaping plates removed. The switch capacitance of Figure A-17 has been replaced by a transmission line and R_4 was added to control the trigger voltage. A capacitive monitor was installed on the ground side of the transmission line approximately 20 inches from the switch and consisted of a 6 inch by 36-inch strip of 1/16-inch aluminum bonded to a 1/8-inch sheet of polyethylene. A series resistor made up of six 810-ohms, 2-watt resistors connected the aluminum to the center conductor of an 81-nsec long RG-214/U cable. The output traces from this monitor are labeled $V_{PULSE-LINE}$ in Figure A-24.

The 10 to 90 percent risetime is estimated from Figure A-24 to be a trace measured maximum of 3 nsec from a scope with a 2.4 nsec response time. This means that the switch voltage fall time is less than 3 nsec.

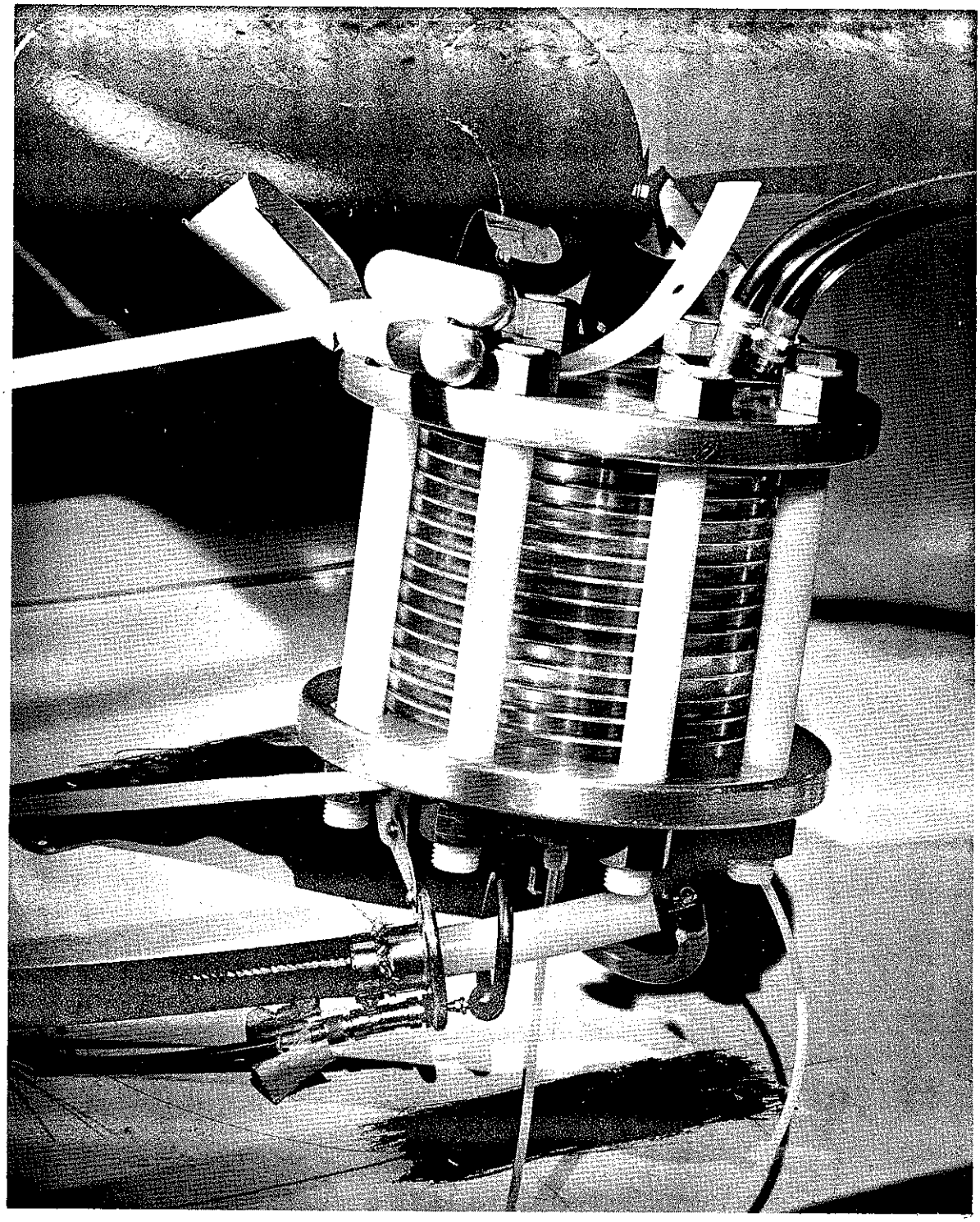

Figure A-23 A top view of the triggered gas switch attached to the oil transmission line in the oil tank.

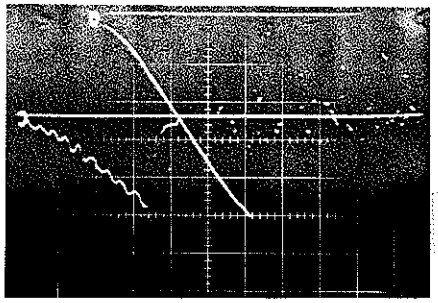

V_{SW}: 0.53 MV/div

V_{TRIG}: 100 kV/div

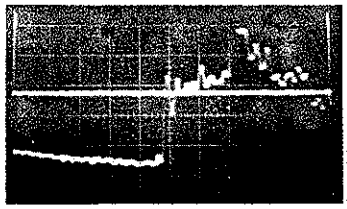

$V_{pulse-line}$

20 nsec/div

a.

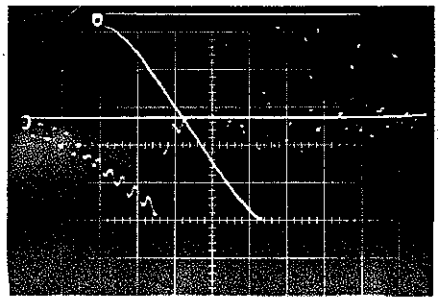

Same as (a)

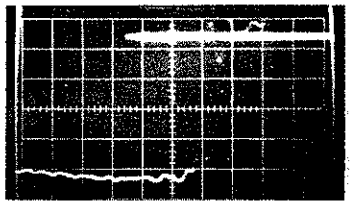

10 nsec/ div

b.

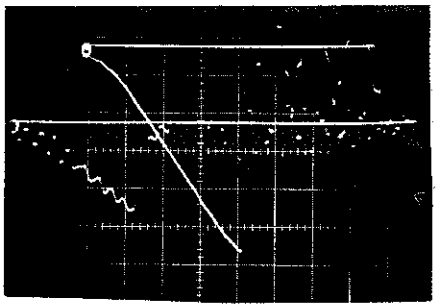

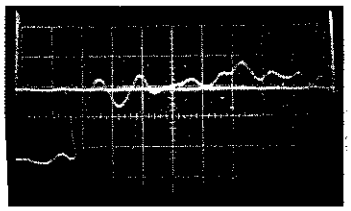

5 nsec/div

c.

Figure A-24 Traces showing the switch voltage, trigger voltage, and pulse line voltage when switching a 60-ohm line.

A series of photographs of the switch is shown in Figure A-25 in the sequence taken. The peak switch voltage is listed in each case. The trigger electrode (ground end of switch) is to the left in these photographs. Each photograph clearly shows multichannel switching. The general absence of looping and the distribution of the channels strongly suggest that the channels are all formed promptly and simultaneously. Shot No. 4 was a self-fire shot and the pulse-line photo was missed. The fall time of shot No. 9 is approximately 3 nsec measured on 5 nsec/div sweep.

The oscilloscope response is 1.4 nsec, 10 to 90 percent, so that the pulse risetime must be less than 3 nsec. (A quadrature summation of risetimes would give a value of 1.8 nsec.) A 3 nsec risetime corresponds to a switch inductance of approximately 85 nH ($2 = RT/2.2$ where T = 10 to 90 percent risetime). This discrepancy from the 150 nH calculated single arc channel switch inductance is explained by the regular multichannel switch operation.

A tabulation of the number of triggered shots attempted is given in Table A-4 for the switch voltage in 100-kV steps. Differentiation is made between the two basic test arrangements, i.e., whether with the 300 ohms series limiting resistor or connected directly to the 60 ohms pulse line.

TABLE A-4

NUMBER OF TRIGGERED SHOTS ATTEMPTED AS A FUNCTION OF VOLTAGE FOR THE TWO BASIC TEST ARRANGEMENTS

Peak Switch Voltage	<2.5	2.5-2.6	2.6-2.7	2.7-2.8	2.8-2.9	2.9-3.0	3.0-3.1	3.1-3.2
# with 300 Ω	32	35	92	58	24	44	33	7
# with 60 Ω	12	2	4	4	4	3	0	0
TOTAL	44	37	96	62	28	47	33	7

Table A-5 is a listing of basic switch dimensions and materials as used in the jitter and risetime tests.

TABLE A-5

Insulators:	
Number	14
Material	Lucite
Thickness	0.5 inch
O.D.	10.00 inches
I.D.	8.00 inches
Gradient Rings:	
Number	13
Material	Al
Thickness	0.125 inch
O.D.	10.50 inch
I.D.	7.62 inch
O-ring groove	0.140 W x 0.077 DP
Tie Rods:	
Material	Nylon
Number	8
Diameter	1.25 inch
Trig Electrode:	
Material	SS303
Diameter	2.75 inches
Top radius	3.0 inches
TESO	0.25 inch
TIG:	
Electrodes	
Material	SS303
Diameter	0.25 inch
Stem	
Material	Brass
Diameter	0.50 inch
Electrode Spacing	0.68 inch
Pressure	75 psig
Electrodes:	
Diameter	4.00 inch
Spacing (Nom)	3.00 inch

TABLE A-5 (cont.)

End Plates:

Material	Al Plate
Thickness	1.25 inch

Gas:

Material	SF_6
Pressure	175 psig

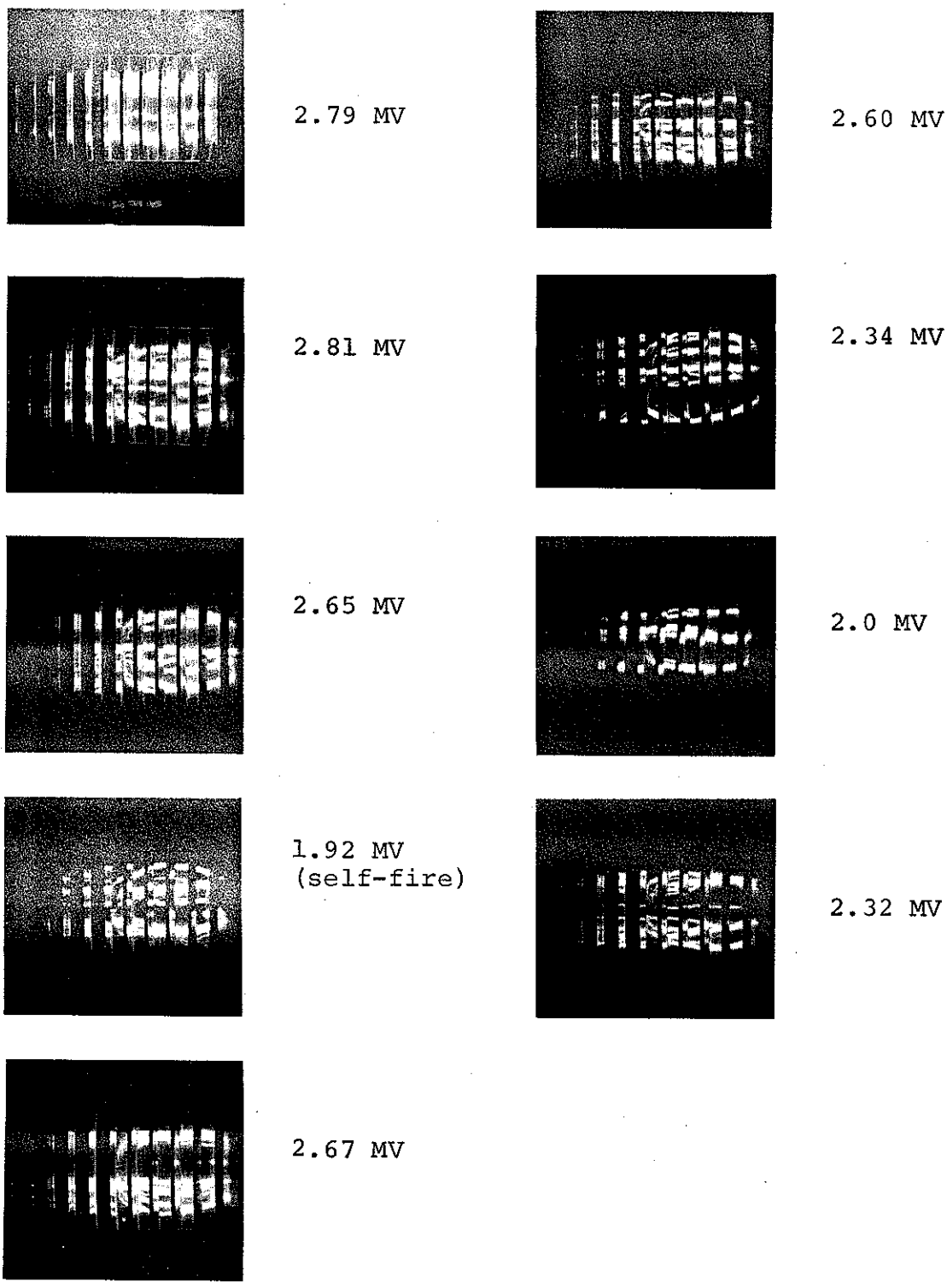

Figure A-25 A sequence of openshutter photographs of the gas switch showing multichannel switching. The peak switch voltage is listed.

APPENDIX B

OIL SWITCH TESTING

SECTION B-1

INTRODUCTION

This report presents the results of the experimental efforts by Physics International Company under contract to Sandia Laboratories for development of a switch to operate in an oil environment.

A three electrode, V/n, open switch was tested in oil for several values of trigger electrode position. The essential elements of the switch consisted of main electrodes formed by 10-inch-diameter semielliptical domes mounted on support plates and a small diameter (1/8 inch) single point trigger electrode. A trigger pulse was derived from either a single pulse line or Blumlein line. In both cases the switching element was a self-closing gas gap. The trigger electrode of the test switch was resistively balanced, and was isolated from the trigger line during pulse charge by another self-closing gas gap, the trigger isolation gap (TIG). The test switch discharged an oil transmission line with series resistance presenting an effective impedance of 100 ohms. Charging was performed by a 39-stage Marx generator.

The best results measured for this switch were for n = 5 with total switch closure times following TIG closure on the order of 48 nsec. A jitter of σ = 2.7 nsec was measured over a voltage range of approximately 1.8 to 2.25 MV peak switch voltage corresponding to values of 70 to 87 percent of self-fire.

SECTION B-2

OIL SWITCH TESTING--PHASE I

The first tests in Phase I were attemps to measure delay and jitter of a single channel triggered oil switch. A basic schematic diagram of the electrical circuit is given in Figure B-1, and a top view of the approximate partial physical layout of the apparatus is given in Figure B-2. A switch line and trigger line were pulse charged from a 39-stage Marx generator. Each line consisted of three parallel 5-inch pipes joined by a 180 degree bend at each end which form the charged electrode. The tank wall is the other side of the line. The oil switch discharged the test switch line through a $CuSO_4$ resistor such that the resistor and line combined presented a 100-ohm impedance. The trigger was initiated by a self-breaking gas trigger gap which, in turn, shorted the trigger line to ground initiating a pulse. At the output end this inverted pulse broke down the trigger isolation gap (TIG) and applied trigger volts to the trigger electrode. The trigger electrode gap isolated the trigger line during pulse charge from the trigger circuit in order that the trigger electrode could be resistively balanced at the potential corresponding to its physical location. The TIG also served as a pulse sharpening gap.

During attempts to trigger with the trigger electrode at V/2 and V/3, it was found that the trigger gap was removing voltage from the switch line back through the resistors from the Marx generator to each line. To reduce this effect, the charging connections were changed as shown by the dotted lines in Figure B-2.

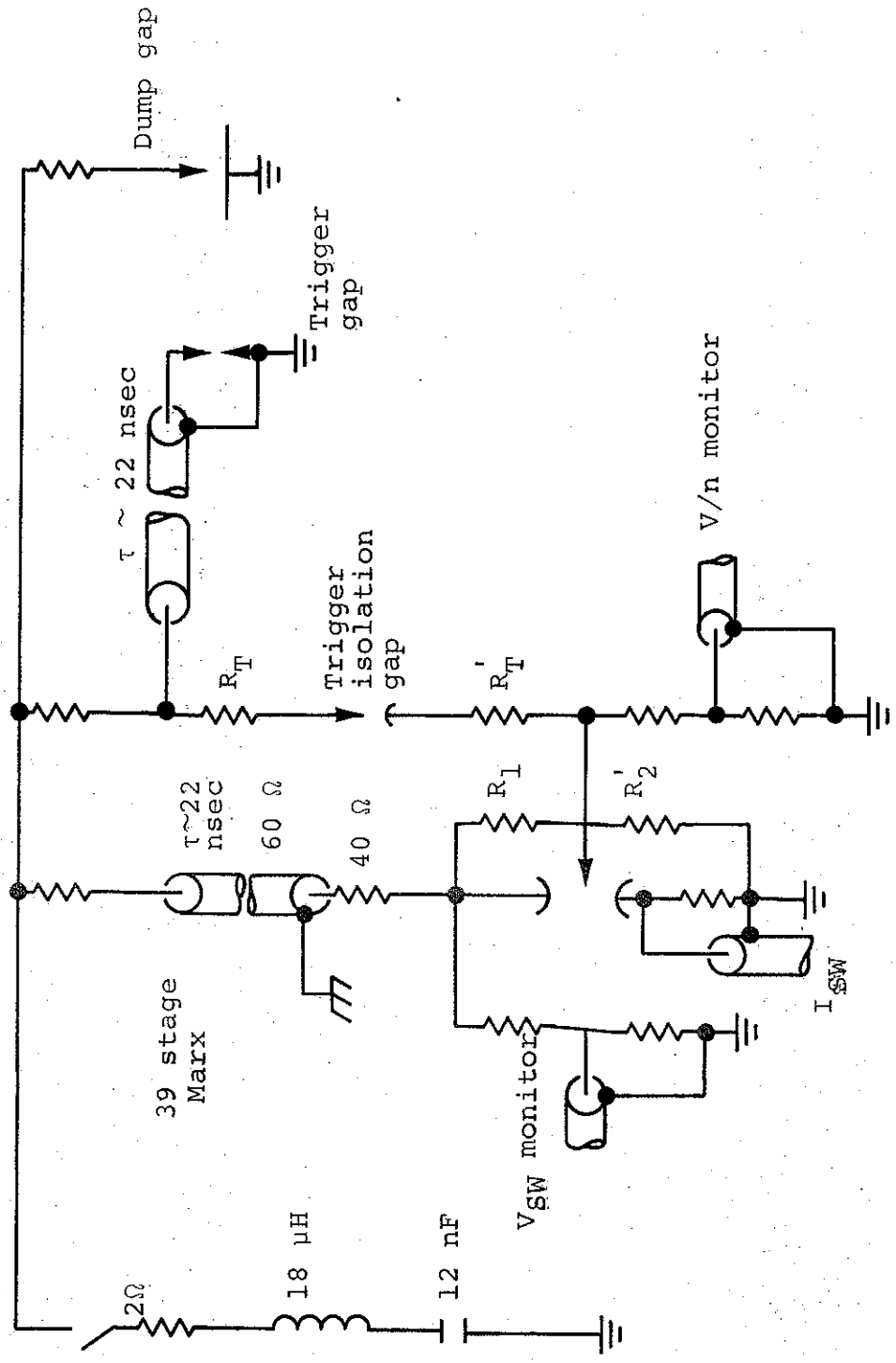

Figure B-1 Basic schematic of oil switch test setup.

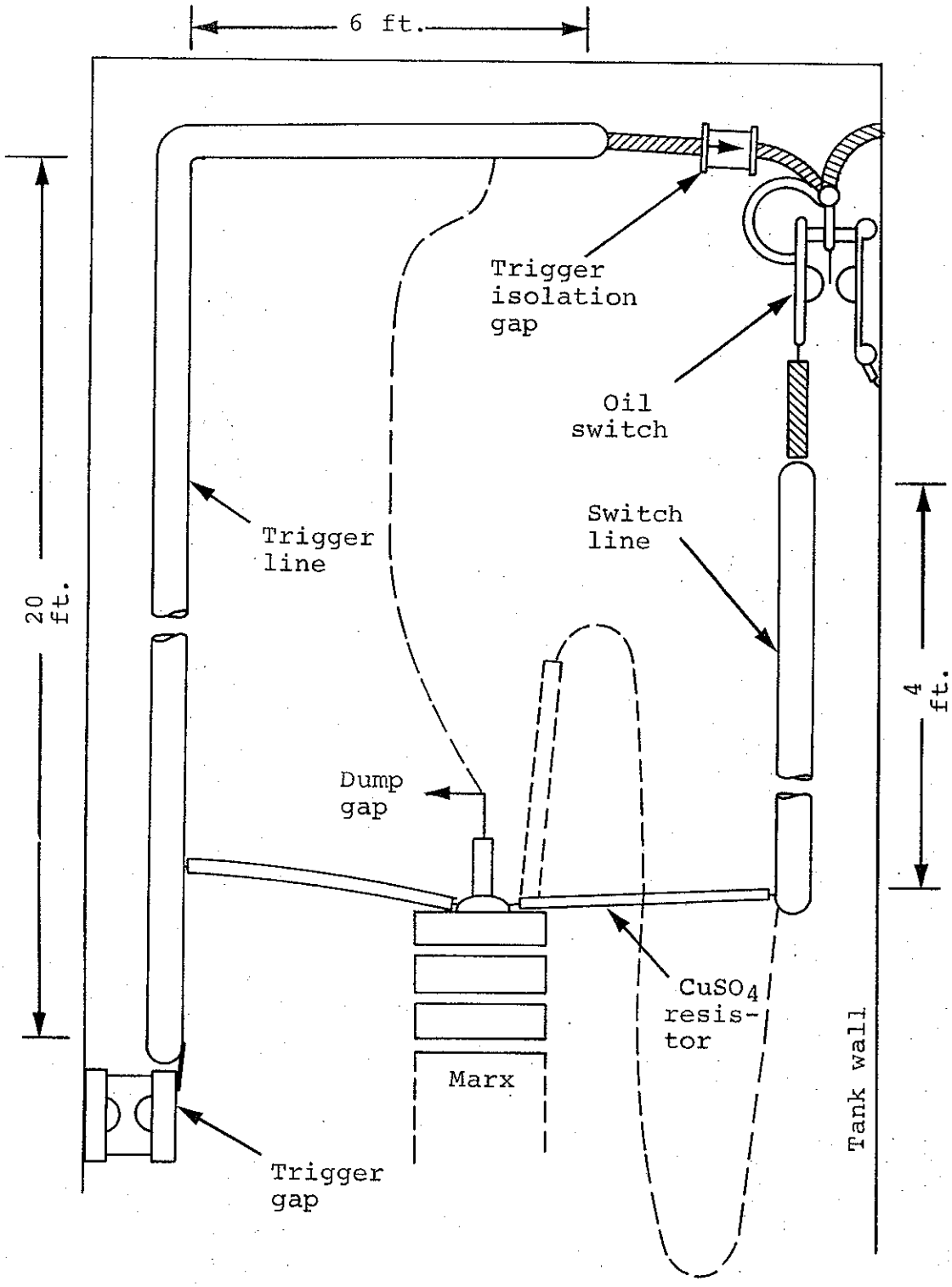

Figure B-2 Physical layout of oil switch test (oil tank--top view).

The pulse charge resistor to the trigger line was eliminated and replaced in function by the dump gap series resistor. The dotted lines of Figure B-2 represent 1/2-inch tubing which was installed to provide transit time isolation between the lines.

Providing the proper balance and trigger resistors was a major task in testing. The schematics of Figure B-3 assume that the TIG has just closed due to arrival of the trigger pulse. It is readily apparent from Figure B-3a that the trigger pulse has its greatest effect on the trigger electrode when the balance resistors R_1 and R_2, (R_2 includes the monitor), are large and R_T is small. In this case the RC time constant of the trigger source impedance ($R_T + Z_T$) and the strays associated with the trigger electrode and resistors are a minimum, as is also the resistive division due to R_2 in parallel with $R_1 + R_o + Z_o$ in series with $R_T + Z_T$.

The circuit of Figure B-3b assumes that closure has occurred in the wide (off ground) side. Now R_1 is shorted out and the switch voltage is applied to the short side of the switch. If R_2 is large the voltage across R_2 or the second switch side is given by

$$v_e = v_o \left\{ \frac{Z_T + R_T - \frac{v_T}{v_o}(Z_o + R_o)}{Z_o + R_o + Z_T + R_T} \right\}$$

This shows that the trigger line and series resistor acts as a load to the switch line and that the second side closure may be degraded by reducing R_T, i.e., it is in conflict with achieving fast first side closure.

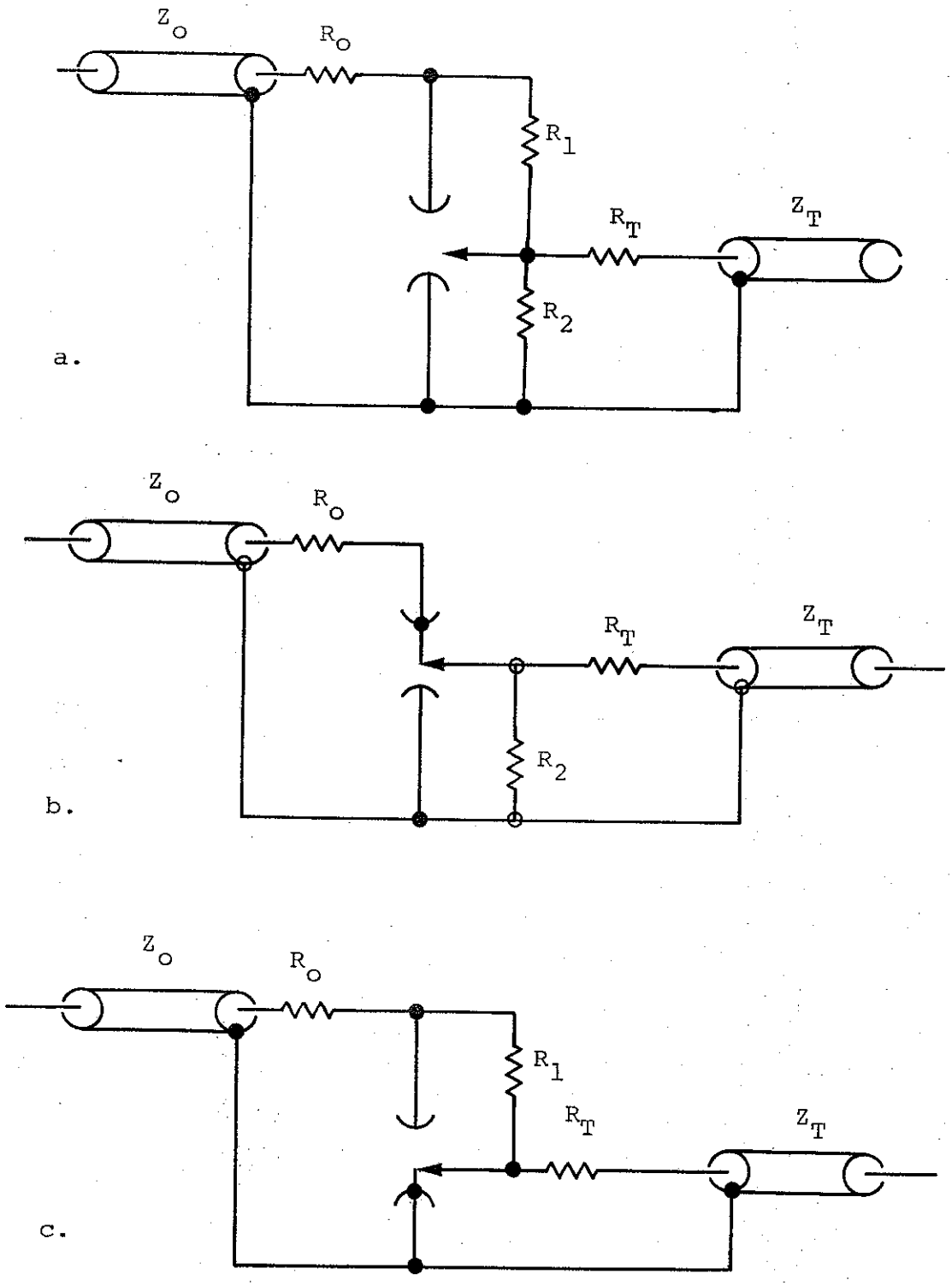

Figure B-3 Switch configurations following TIG closure (a), wide side closure (b), and short side close (c).

The circuit of Figure B-3c assumes the ground side of the switch closed first. In such event, the remaining switch voltage is determined by the resistive divider Z_o, R_o, and R_1 and is given by

$$v_e = v_o \left(\frac{R_1}{R_1 + R_o + Z_o} \right).$$

Note that the trigger pulse polarity is such that the voltage of the ground side of the switch is first removed and then reversed in polarity so that this mode of switching is most apt to occur for large values of n, i.e., small spacings and the wide side must close with less than full switch voltage over most of the switch spacing.

The values of R_1 and R_2 are limited by the requirement that the stray capacitance of the switch electrode and attachments must be charged in times that are short compared to the pulse charge time.

Noise on monitor traces was a major problem that made resolution of time data difficult.

The switch electrodes were 10-inch diameter semi-elliptical steel heads welded to flat plates for mounting and spacing. The trigger electrode was a 0.125-inch-diameter stainless steel rod extending 8 inches from a 1-inch-diameter steel stem. The latter was mounted in a hole through a Lucite block clamped between the electrode backup plates. The stem was mounted in the center of the plates and trigger electrode-to-dome spacing was adjusted

by bending the electrode sharply near the stem and gradually over the remainder in an attempt to approximate field lines near the domes. The electrode tip ended approximately 1 inch from the center of the domes. The tip was ground over a distance of about 1 inch to a point of less than 1/32-inch diameter.

The V/n monitor is the principal source of timing data included in this report. Note that it forms, in fact, a portion of the balance divider and so reads proportional to total switch voltage until the TIG or one side of the switch closes. It should be noted that if the wide side of the switch closes first, for example, the monitor should show a change of n times in amplitude neglecting other loading.

Traces for two shots are given in Figure B-4 for n = 3. The measured switch spacings were 2.15-inches dome-to-dome at the center and 0.7-inch electrode edge-to-ground dome and 1.4-inches electrode edge-to-floating dome. The resistor between TIG and trigger (R_T') was eliminated by now and the value of R_T was set at 390 ohms. R_1 was 3.0 kΩ and the parallel combination of R_2' and monitor was 1.5 kΩ. Oil switch self-break was measured at 2.5 to 2.7 MV for these spacings.

The traces in Figure B-4 are interpreted to give in (a) V_{SW} = 1.97 MV, closure of the first side 40 nsec, total switch closure 61 nsec and by difference, second side closure is 21 nsec. The respective values in (b) are 2.02 MV, 43 nsec, 64 nsec, and 21 nsec.

The initial trace of the V/n monitor is negative with the electrode voltage being one-third the switch voltage. When the trigger pulse arrives, it is capacitively coupled to the switch

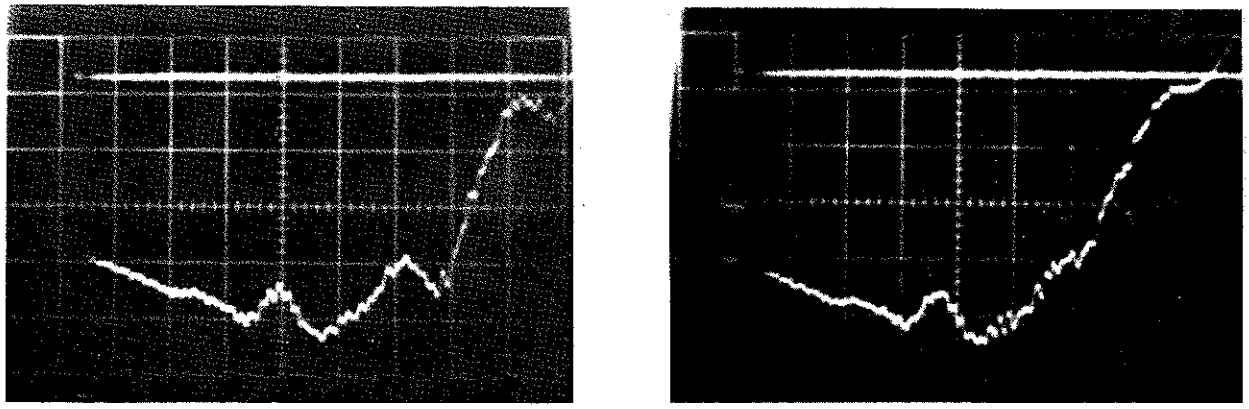

(a) (b)

V_{sw} Monitor
Vertical: 0.43 MV/div
Horizontal: 20 nsec/div

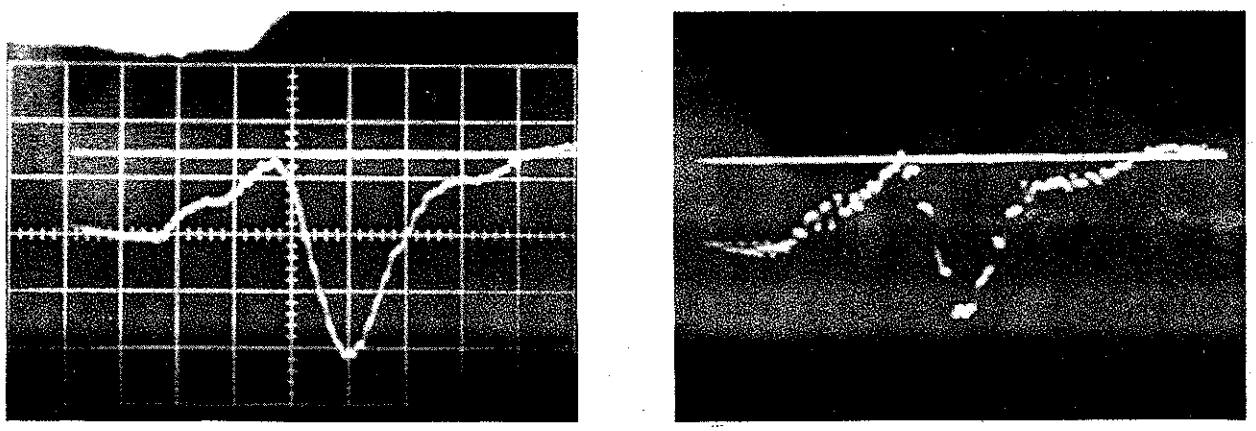

(a) (b)

V/3 Monitor

Vertical: 1.18 MV/div
Horizontal: 20 nsec/div

Figure B-4 Switch and trigger electrode monitor waveforms for two shots. Switch spacing dome to dome measured 2.15 inches. Electrode to domes, measured 0.7 (from ground) and 1.4 inches.

and electrode causing a positive going charge followed by the start of recovery when the TIG closes. At this point the electrode tends to be even more positive until breakdown to the negative charge wide side occurs when the electrode is pulled negative again. Second half closure (short or ground side) takes all test switch electrodes to ground except for switch inductive and resistive effects. First side closure is taken as the time from arrival of the trigger pulse, (capacitively fed through) (first plus going break), to the negative going break leading to the larger excursion. Total closure is measured from trigger pulse arrival to second side closure. Thus the TIG closure jitter is included in the data for first side and overall closures. The switch monitor shows the effect of capacitive trigger pulse coupling but the voltage recovers until the TIG closes and the resistive division starts taking voltage off the switch. The second negative going hitch may be due to pulse line or trigger pulse line reflections. The values of voltage stated in the data plots are the peak value measured following recovery from the capacitively feedthrough trigger pulse. The slow fall time shown by V_{SW} monitor traces (Figures B-4, B-5, and B-6) are due to the $CuSO_4$ monitors. (In tests of the gas switch where other parameters were established, a capacitive monitor was used to measure fall time on the switched pulse line.)

Data for the V/3 switch is plotted in Figure B-7a in which the breakdown time is plotted for first side, second side, and total closure as a function of voltage. Attempts were made to fire at particular voltage by maintaining the Marx voltage and pressure constant, but scatter was introduced by trigger gap jitter. The values of σ given are calculated from the spread from the ruled line, the latter an estimated best fit. There are five more data points on total switch closure than for

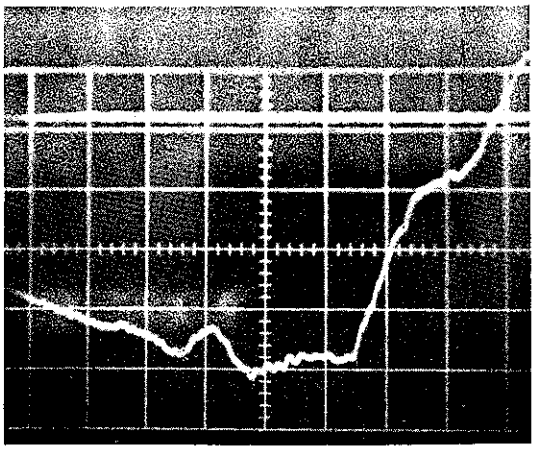

V_{sw}

Vertical: 0.45 MV/div
Horizontal: 20 nsec/div

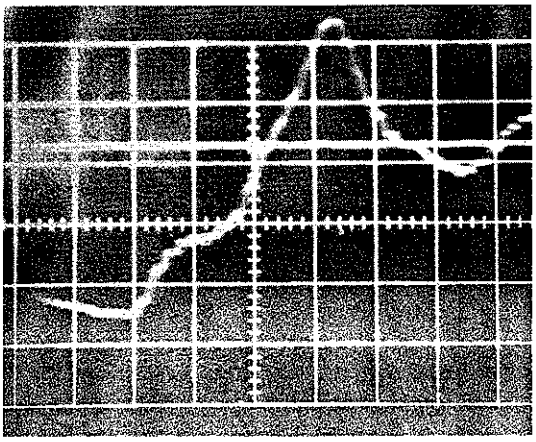

V/5

Vertical: 0.65 MV/div
Horizontal: 20 nsec/div

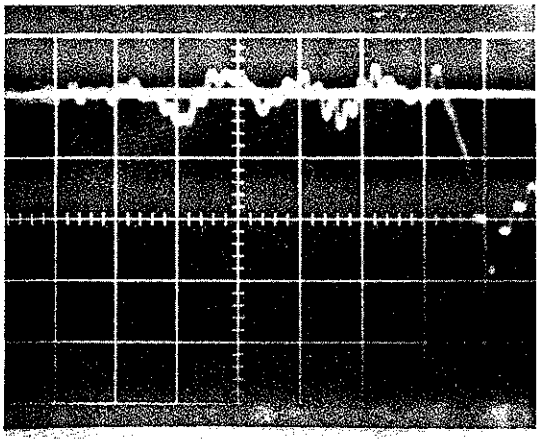

I_{sw}

Vertical: Not calibrated
Horizontal: 10 nsec/div

Figure B-5 Typical trace for V/5 electrode triggering.

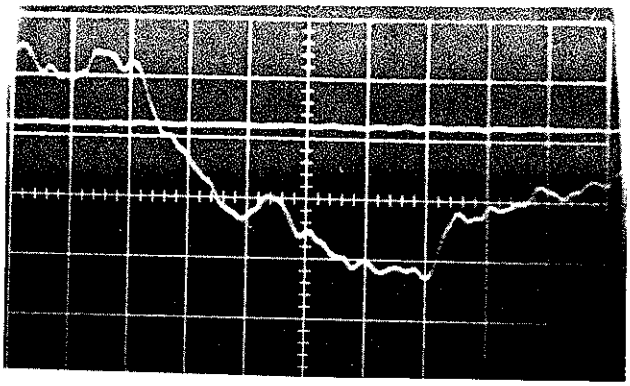

V_{trig}

Horizontal: 10 nsec/div

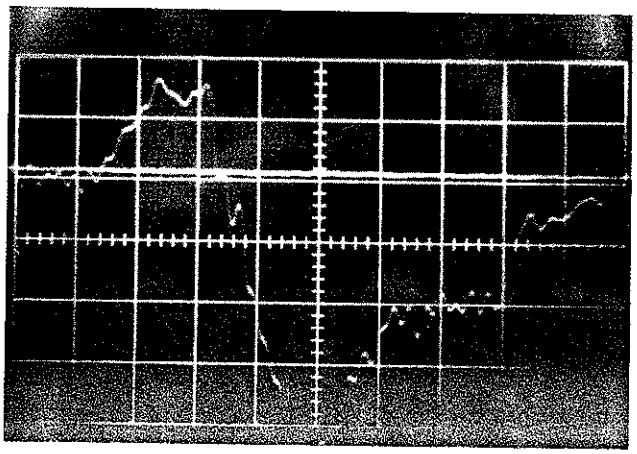

V/n

Horizontal: 10 nsec/div

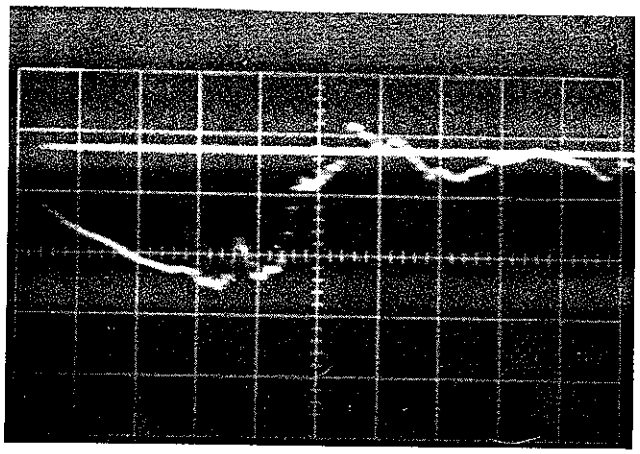

V_{sw}
Vertical: 1.0 MV/div
Horizontal: 50 nsec/div

Figure B-6 Typical traces for Blumlein line triggering.

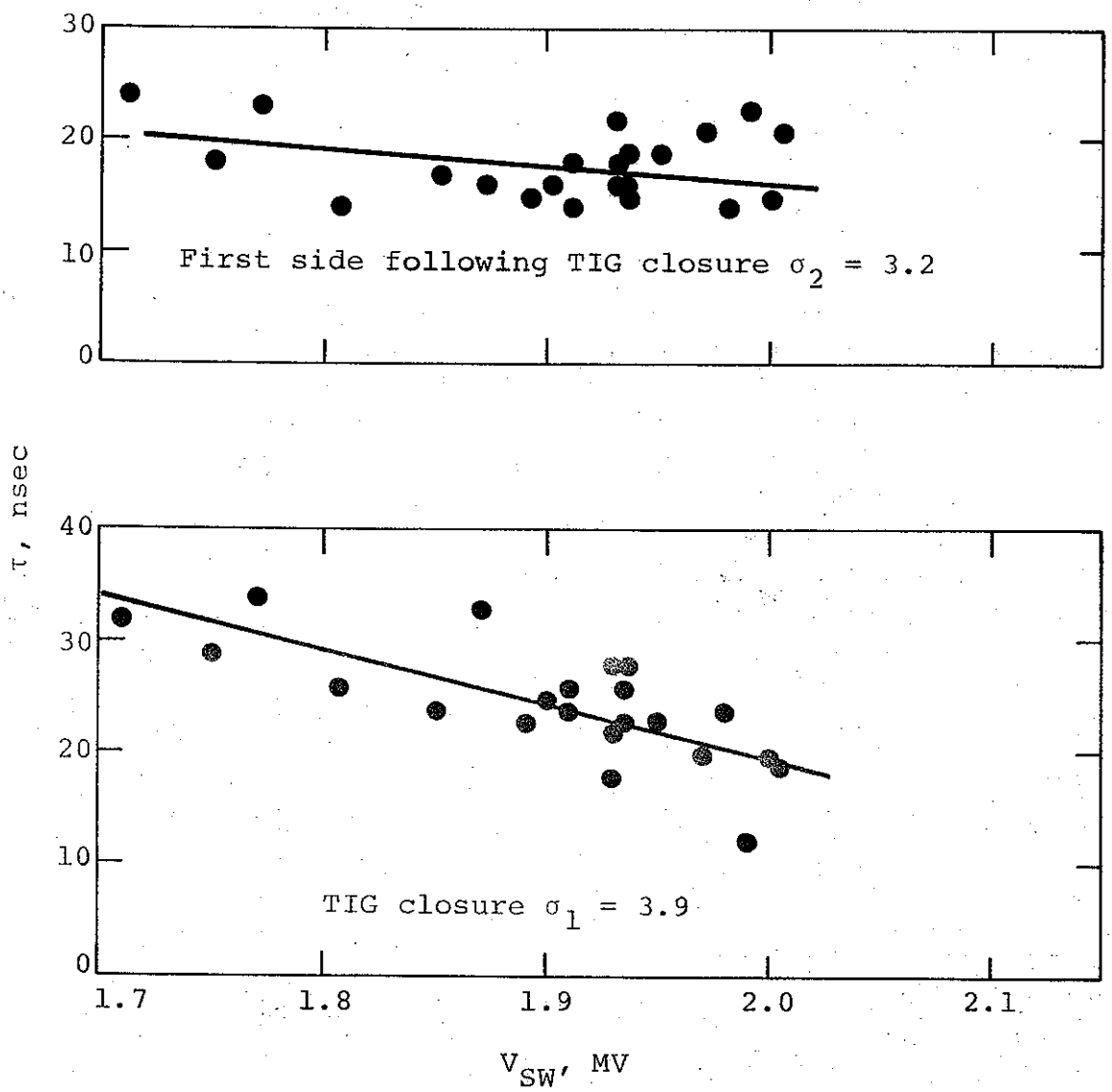

Figure B-7 Closure times (τ) of the TIG and first side of the switch for n = 3.

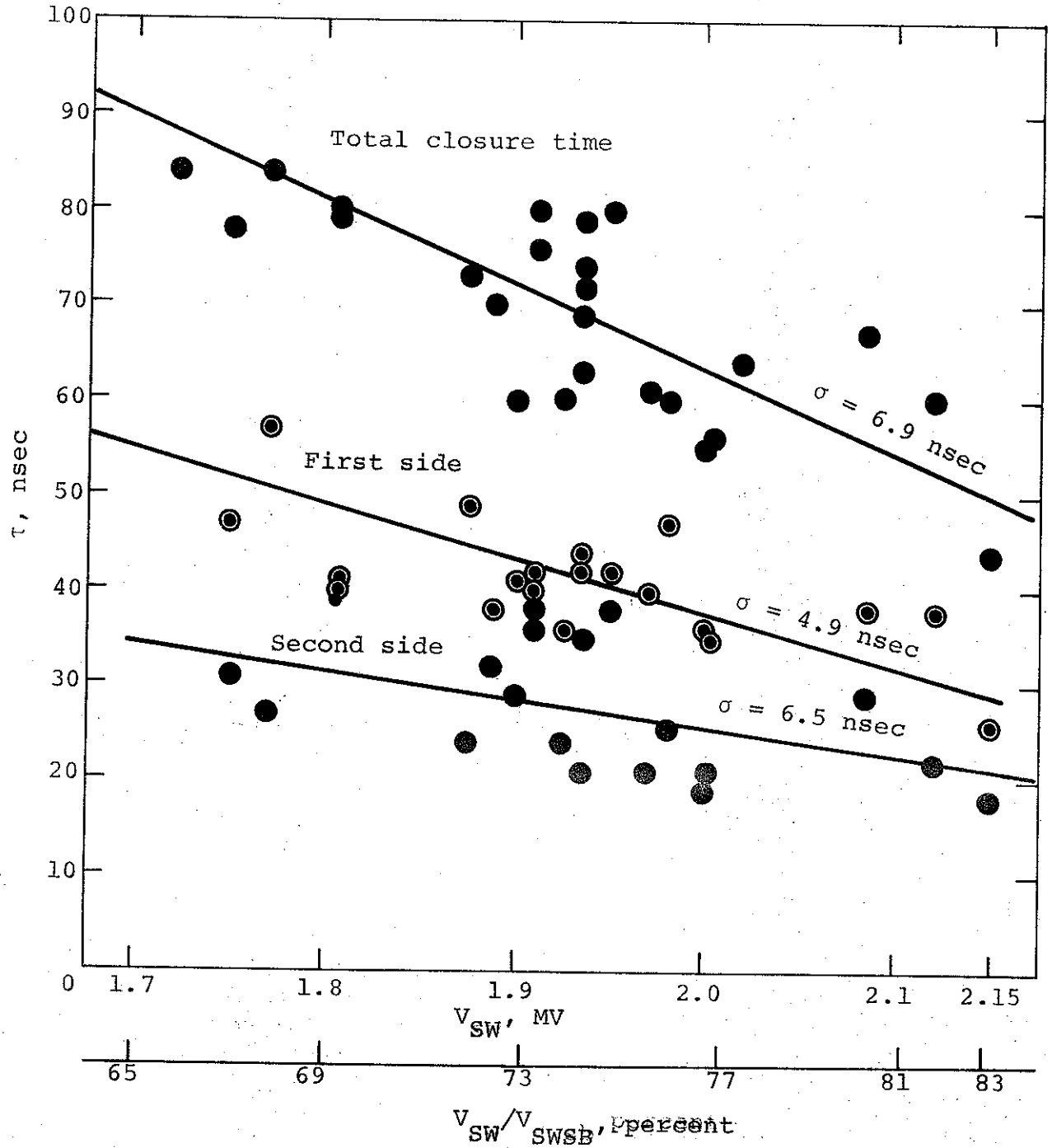

Figure B-7a Closure times (τ) of the triggered oil switch for V/3 setting for various peak switch voltages and percentage of self-fire.

single side closures representing data points that the total could be reasonably well read. However the break following first side closure was too rounded to be read with confidence. Figures B-7b and Figures B-8b for n = 4 give plots for best estimates of TIG closure and first side closure. The sum of the two closures is typically read within ± 2 nsec at each breakpoint for a total spread of 8 nsec while the reading of TIG closure is probably as great as ± 4 nsec on many traces for a possible spread of 12 nsec. Since the probable sum error is less than the error in reading either part, it is only fortuitous that the root mean square value of the mean deviations for the V/3 case corresponds closely to the mean deviation of the measured sum; whereas for the V/4 case the root mean square value of the mean deviation is substantially greater, thus indicating the greater probable error in reading the TIG closure value.

The electrode spacings for n = 4 were reset to nominally 0.5 inch and 1.5 inches. The balance divider consisted of R_1 = 7.5 kΩ and R_2 = 2.5 kΩ (the monitor). Waveshapes were quite similar to the V/3 and data are plotted in Figure B-8a.

The electrodes for n = 5 were next set at 0.4 inch and 1.6 inches with the balance divider made up of R_1 = 10 kΩ and R_2 = 2.5 kΩ. The traces of Figure B-5 are typical of this series, and data are plotted in Figure B-9, but in this case do not include the TIG time. The trace labeled I_{SW} is from a resistive-inductive monitor connected between the ground side electrode and tank ground. Comparison of a number of traces led to the conclusion that the start of the trace is roughly coincident with the trigger pulse feedthrough, and the positive break is the closure of the TIG. The large negative excursion is the closure of the oil switch. Time measurements made on any particular shot are

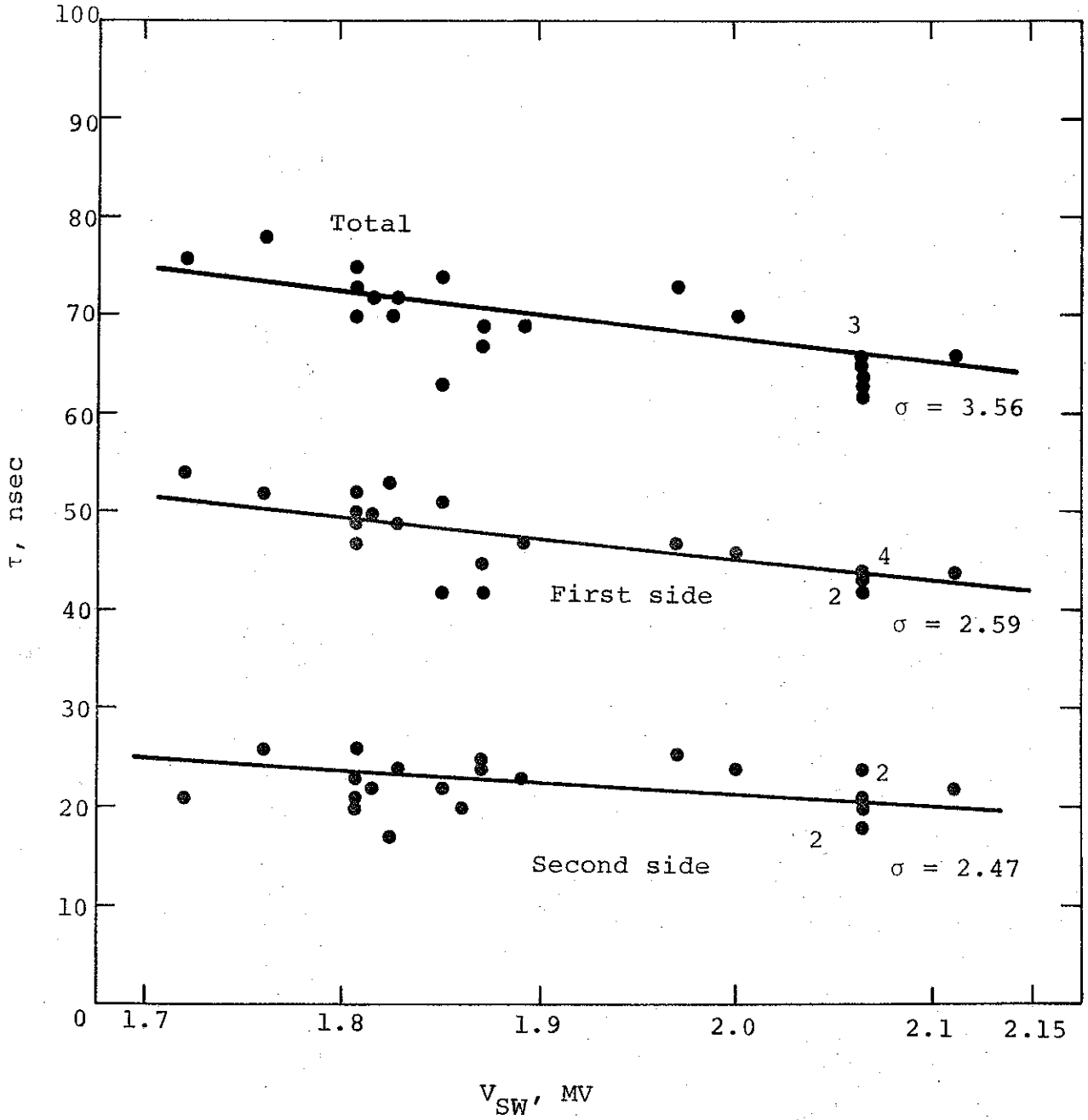

Figure B-8a Closure times (τ) for triggered oil switch for V/4 setting.

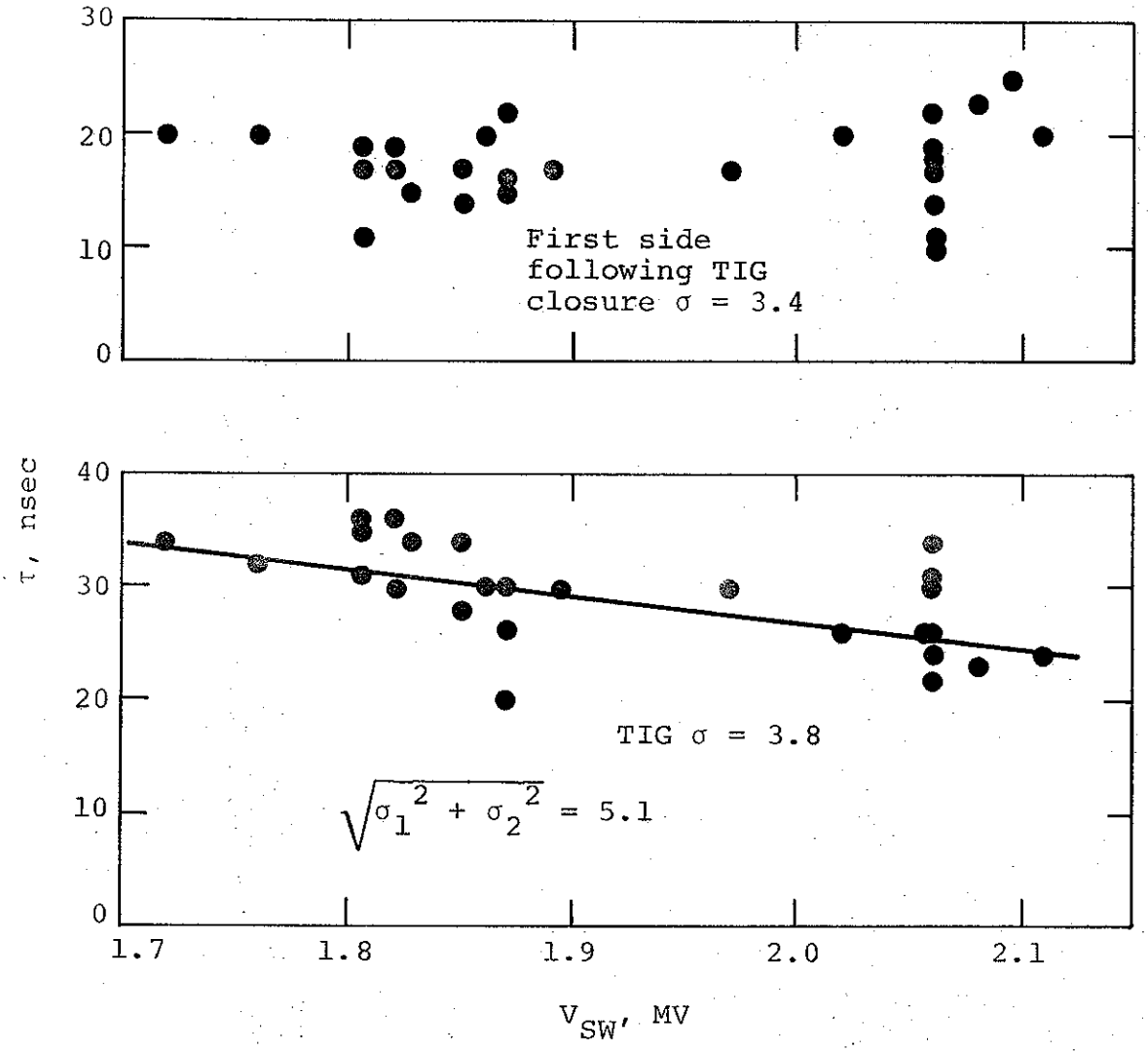

Figure B-8b Closure time (τ) of the TIG and first side of the switch for n = 4.

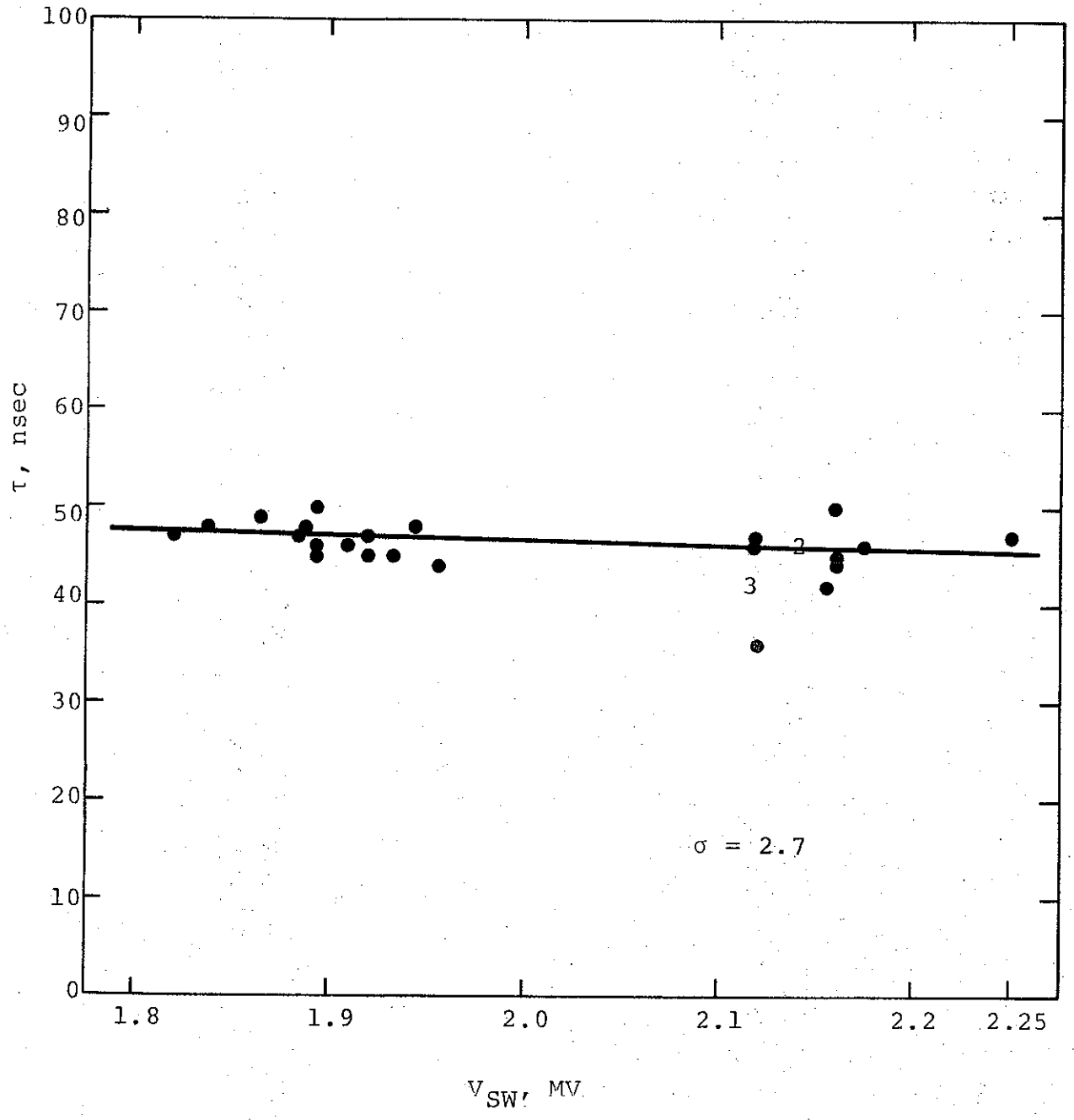

Figure B-9 Closure times τ of the triggered oil switch for V/5 setting (overall time only).

perhaps within 6 nsec of recorded value, but consistency in reading from trace to trace is somewhat less. This series was characterized by the closure of the switch on the positive excursion of the trigger pulse suggesting that second (short) side closure is very rapid or nearly coincident with the wide side closure. Data in Figure B-9 are for total closure only, but do not include TIG jitter as the traces are interpreted.

The next step in testing was to try to increase the trigger pulse amplitude by changing the trigger pulse line into a Blumlein line source. The traces of Figure B-6 were taken as the most informative set. The top trace is taken from a monitor attached to the output end of the trigger Blumlein line. The middle trace shows the V/n monitor with the TIG breaking at 1.4 divisions on scale. At 3.2 divisions, the wide side closes and switch closure completes at 5.3 divisions. Data according to this interpretation are plotted in Figure B-10.

The trigger electrode was next sharpened to a fine point and the series repeated. Data are plotted in Figure B-11.

The jitter in measured closure times for the oil switch was significantly greater than the test objective of $\sigma < 1$ nsec, even for the case of $n = 5$ where the first and second sides appeared to close nearly simultaneously. Several ways of improving oil switching were suggested. These included (1) operating with a more uniform switch field obtainable through electrodes with a larger radius but with increased fields near the center, (2) reducing trigger losses by providing more trigger pulse but arranging to reduce the effect on switch voltage due to first side closure, (3) an electrode with a smaller radius, and (4) use of an edge instead of a point trigger electrode.

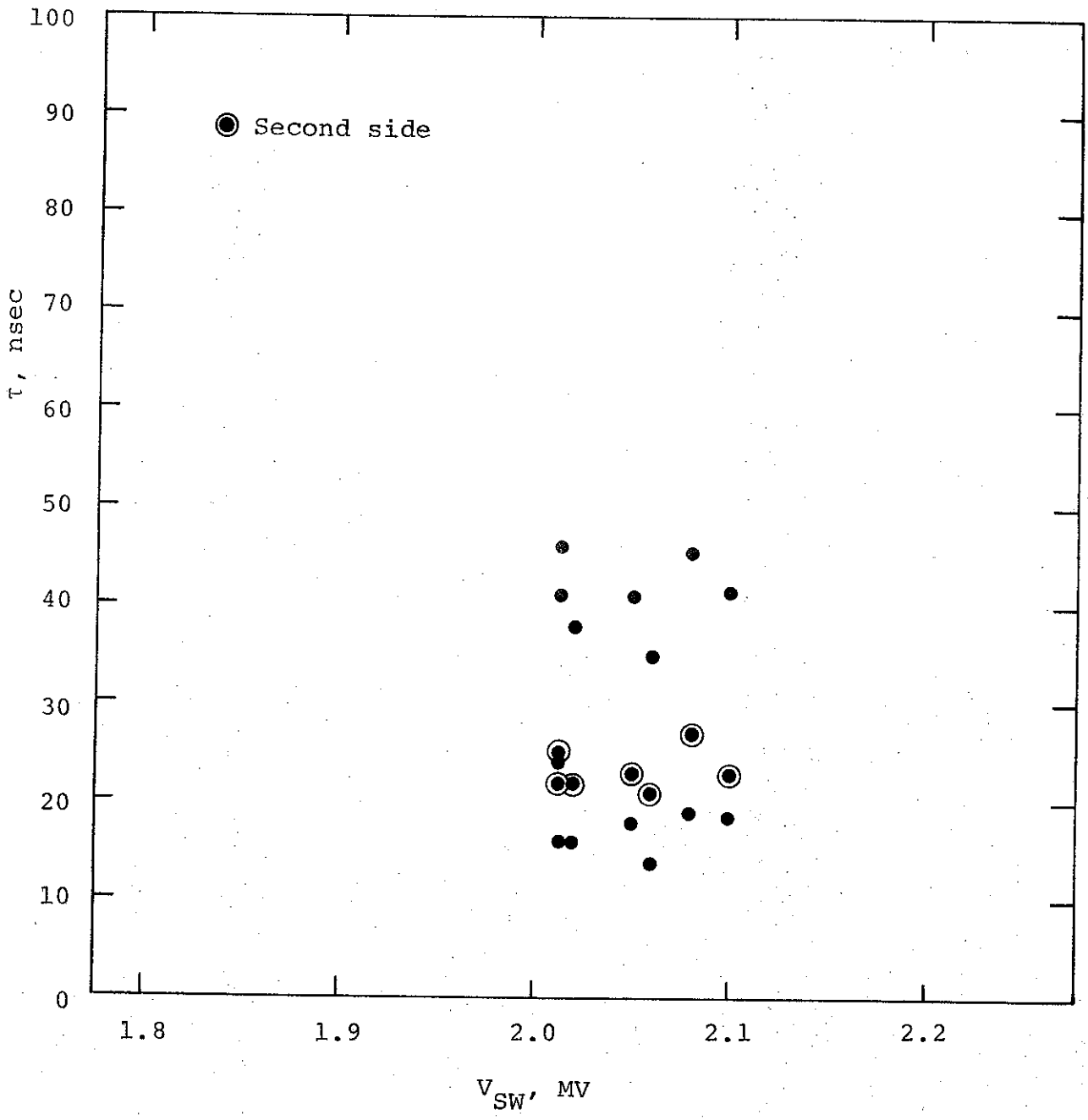

Figure B-10 Closure times (τ) for Blumlein line triggered oil for V/5 setting.

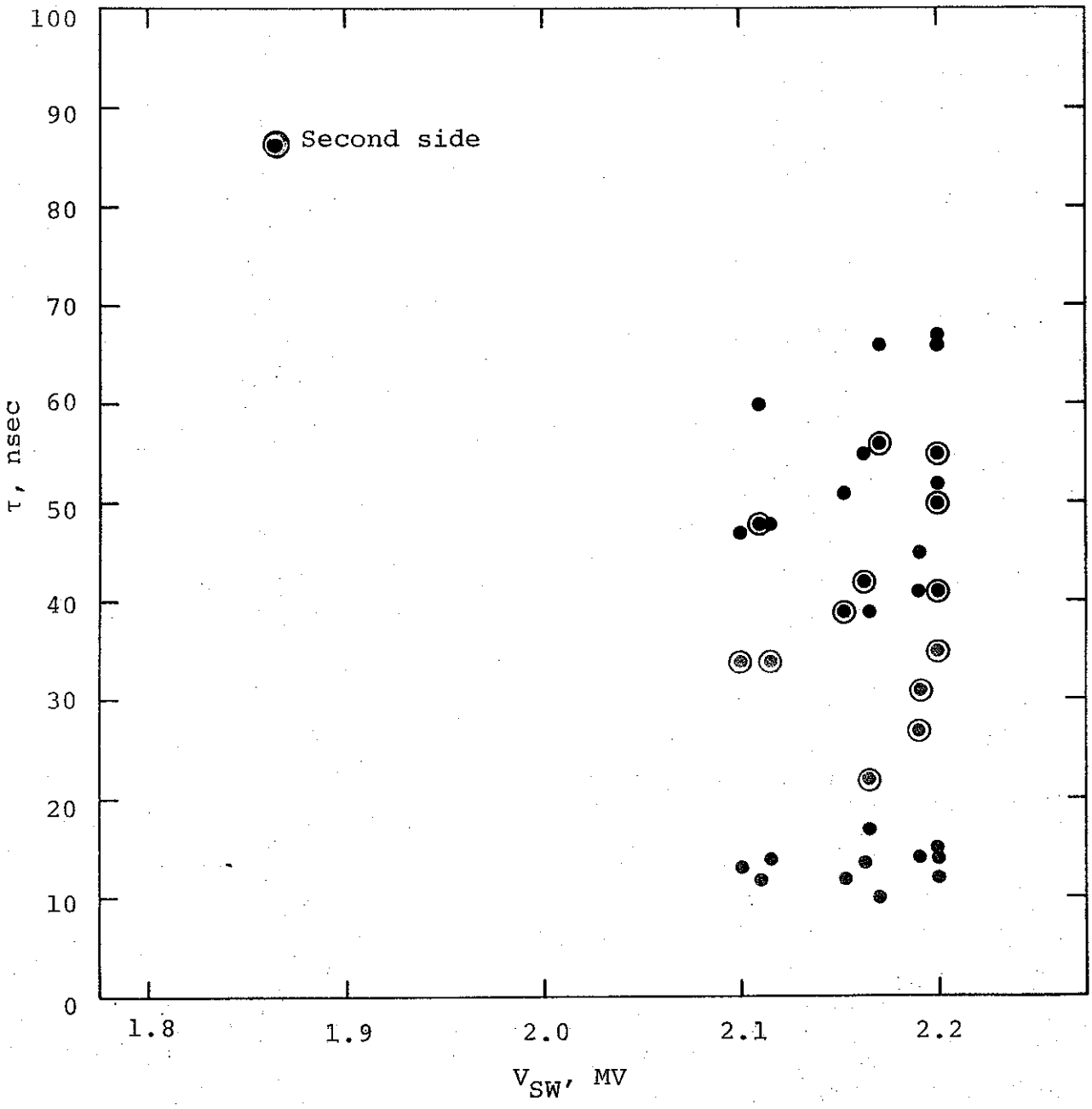

Figure B-11 Closure times (τ) for Blumlein line triggered switch for V/5 setting with a sharpened trigger electrode.

Sandia Corporation was simultaneously working on an oil switch and to prevent duplication of effort and to provide a viable backup, Physics International Company was directed to proceed with the gas dielectric portion of the contract.

ADDENDUM

Costs of producing production type quantities of switches were obtained as part of Contract 14-1027. Methods of fabrication were discussed with vendors to establish the most economical switch costs, and the information given in this addendum to PIFR-605 is based on vendor quotes and estimates of inflationary increases covering a period of three to twelve months.

Switches identical to the latest modification of the switch tested under the above contract are priced in quantities of 10, 50, and 100 each with respective estimated unit prices of $2700, $1800 and $1500. This price is FOB San Leandro. It includes procurement of parts, quality control, assembly, pressure check, and shipping preparation. These items are listed as a percent of total costs.

The tabular listing of costs shows that no single part dominates the cost and that significant gains might be expected only through careful attention to all parts and assembly procedures.

TABLE I

DISTRIBUTION OF SWITCH PARTS COSTS GIVEN AS A PERCENT OF TOTAL FOR QUANTITIES OF 10, 50, AND 100 SWITCHES

Item	Quantity Switches		
	10	50	100
Insulator rings	10.2	13.5	14.3
Gradient rings	19.1	22.4	20.4
Tie rods	3.1	4.7	5.5
End plates	9.3	12.8	12.6
Solid electrode	2.0	2.8	3.1
Trigger electrode assembly	13.8	18.5	19.5
Trigger isolation gap	2.0	2.9	3.0
Miscellaneous parts	2.9	1.3	1.2
PI labor	37.6	22.2	20.4